

Water Resources Research

RESEARCH ARTICLE

10.1029/2018WR022612

Key Points:

- Dissolved nitrogen in groundwater provides a means to differentiate high- and low-flux infiltration of stray gas
- Nitrogen concentrations and isotope values may attribute natural gas sources

Correspondence to:

T. E. Larson,
toti.larson@beg.utexas.edu

Citation:

Larson, T. E., Nicot, J.-P., Mickler, P., Castro, M. C., Darvari, R., Wen, T., & Hall, C. M. (2018). Monitoring stray natural gas in groundwater with dissolved nitrogen. An example from Parker County, Texas. *Water Resources Research*, 54. <https://doi.org/10.1029/2018WR022612>

Received 11 FEB 2018

Accepted 7 AUG 2018

Accepted article online 15 AUG 2018

Monitoring Stray Natural Gas in Groundwater With Dissolved Nitrogen. An Example From Parker County, Texas

Toti E. Larson¹ , Jean-Philippe Nicot¹ , Patrick Mickler¹, M. Clara Castro² , Roxana Darvari¹, Tao Wen^{2,3} , and Chris M. Hall²

¹Bureau of Economic Geology, The University of Texas at Austin, Austin, TX, USA, ²Department of Earth and Environmental Sciences, University of Michigan, Ann Arbor, MI, USA, ³Earth and Environmental Systems Institute, Pennsylvania State University, University Park, PA, USA

Abstract Concern that hydraulic fracturing and natural gas production contaminates groundwater requires techniques to attribute and estimate methane flux. Although dissolved alkane and noble gas chemistry may distinguish thermogenic and microbial methane, low solubility and concentration of methane in atmosphere-equilibrated groundwater precludes the use of methane to differentiate locations affected by high and low flux of stray methane. We present a method to estimate stray gas infiltration into groundwater using dissolved nitrogen. Due to the high concentration of nitrogen in atmospheric-recharged groundwater and low concentration in natural gas, dissolved nitrogen in groundwater is much less sensitive to change than dissolved methane and may differentiate groundwater affected high and low flux of stray natural gas. We report alkane and nitrogen chemistry from shallow groundwater wells and eight natural gas production wells in the Barnett Shale footprint to attribute methane and estimate mixing ratios of thermogenic natural gas to groundwater. Most groundwater wells have trace to nondetect concentrations of methane. A cluster of groundwater wells have greater than 10 mg/L dissolved methane concentrations with alkane chemistries similar to natural gas from the Barnett Shale and/or shallower Strawn Group suggesting that localized migration of natural gas occurred. Two-component mixing models constructed with dissolved nitrogen concentrations and isotope values identify three wells that were likely affected by a large influx of natural gas with gas:water mixing ratios approaching 1:5. Most groundwater wells, even those with greater than 10-mg/L methane, have dissolved nitrogen chemistry typical of atmosphere-equilibrated groundwater suggesting natural gas:water mixing ratios smaller than 1:20.

Plain Language Summary Hydraulic fracturing, horizontal drilling, and associated natural gas production have dramatically changed the energy landscape across America over the past 10 years. Along with this renaissance in the energy sector has come public concern that hydraulic fracturing may contaminate groundwater. In this study we measure the chemistry of dissolved gas from shallow groundwater wells located above the Barnett Shale natural gas play, a tight gas reservoir located west of the Dallas-Fort Worth Metroplex. We compare groundwater chemistry results to natural gas chemistry results from nearby production wells. Most groundwater wells have trace to nondetectable concentrations of methane, consistent with no measurable infiltration of natural gas into shallow groundwater. A cluster of groundwater wells have greater than 10 mg/L dissolved methane concentrations with alkane chemistries similar to natural gas. Using dissolved nitrogen and alkane concentrations and their stable isotope ratios in combination with chemical mixing models, we conclude that natural gas transported from the shallower Strawn Group affected these groundwater wells rather than natural gas from the deeper Barnett Shale, which is the target of hydraulic fracturing in this area. These results suggest that hydraulic fracturing has not affected shallow groundwater drinking sources in this area.

1. Introduction

Unconventional natural gas extraction occurs near municipalities including the Dallas-Fort Worth metroplex, and this has increased public awareness about the potential for groundwater contamination associated with hydraulic fracturing. Horizontal drilling and hydraulic fracturing technologies are used to increase permeability in shale and tight formations. There is concern that hydraulic fracturing will cause natural gas, reservoir brines, and associated hydraulic fracturing fluids to migrate from natural gas reservoirs to shallower

groundwater aquifers (<250-m depth) thereby threatening drinking water supplies (Christian et al., 2016; Jackson et al., 2013; Osborn et al., 2011; Thompson, 2012). Geochemical studies in the Marcellus Shale of Pennsylvania, the Utica Shale of New York State, and the Barnett Shale, Eagle Ford Shale, and Haynesville Shale of Texas have attributed methane in shallow groundwater to either deep thermogenic *stray* or shallow low-temperature microbial sources (Christian et al., 2016; Darrah et al., 2014; Jackson et al., 2013; Molofsky et al., 2013; Nicot et al., 2017; Osborn et al., 2011; Siegel et al., 2015; Wen et al., 2015, 2016). Here the phrase *stray gas* refers to natural gas, of an undetermined origin, that is encountered unexpectedly in shallow groundwater aquifers. Source attribution techniques for stray gas commonly employ concentration ratios of methane, ethane, and propane and their stable carbon and hydrogen isotope ratios (i.e., Bernard and Schoell plots; Bernard et al., 1977; Grossman et al., 1989; Prinzhofer et al., 2000; Rostron & Arkadaskiy, 2014; Schoell, 1980; Whiticar, 1999). Bernard and Schoell plots can effectively differentiate microbial and thermogenic sources of methane because low-temperature methanogenesis generates methane with a carbon isotope value that is lower than methane derived from thermogenic processes, and thermogenic natural gas typically contains appreciable amounts of ethane and propane (Bernard et al., 1977; Grossman et al., 1989; Prinzhofer et al., 2000; Schoell, 1980). Attribution with alkane chemistry is complicated by the potential for mixing of multiple sources of thermogenic natural gas of different maturity with additional sources of microbial methane (Moritz et al., 2015; Zhang et al., 1998). In addition to mixing of multiple sources, anaerobic methane oxidation is a common groundwater process that can modify the carbon isotope values and relative concentrations of residual dissolved alkanes (Barker & Fritz, 1981; Zhang et al., 1998) and dissolved inorganic carbon (DIC; Barker & Fritz, 1981; Grossman et al., 1989; Zhang et al., 1998). To a lesser degree, carbon isotope values of methane and alkane ratios may be affected by transport and migration, but these effects are likely small (Fuex, 1980; Lu et al., 2015; Prinzhofer et al., 2000). For these reasons, additional geochemical tools including dissolved noble gases, which can provide further insight into methane source attribution and identify possible transport mechanisms of stray gas, has been applied to natural gas migration studies.

Dissolved noble gas concentrations and their isotope ratios are used to estimate groundwater recharge temperatures (Solomon et al., 1996) and to trace crustal fluid processes such as gas-phase transport through water saturated media (Ballentine et al., 2002; Darrah et al., 2014; Gilfillan et al., 2009; Wen et al., 2016). These efforts take advantage of differences in crustal, mantle and atmosphere noble gas concentrations and isotope ratios along with the inert behavior of noble gases, which are largely unaffected by subsequent microbial processes and reaction with geologic substrate (Ballentine et al., 2002). Ballentine et al. (2002) establishes the fundamental relationships that govern noble gas fractionation during single- and two-phase transport, with a specific focus on solubility effects. Related to natural gas transport, exchange or fractionation of gases between gas- and aqueous phases occurs when a stray gas phase comes into contact with an aqueous phase. Exchange of chemical components between the gas and aqueous phase may add *excess* or remove *strip* dissolved gases from groundwater depending on the degree of gas-water interaction, concentration gradients, temperature, and Henry's Law constants (Ballentine et al., 2002; Cey et al., 2009). Three studies report dissolved noble gas isotopes to evaluate elevated natural gas in shallow groundwater wells from the Barnett Shale of Texas (Darrah et al., 2014; Wen et al., 2016, 2017) and the Marcellus Shale of Pennsylvania (Darrah et al., 2014). Within the Barnett Shale, these studies identify a spatial cluster of groundwater wells that contain high concentrations of natural gas and conclude that the natural gas is likely sourced from the Strawn Group that is stratigraphically above the Barnett Shale, which is the target of hydraulic fracturing (Darrah et al., 2014; Wen et al., 2016, 2017). Nicot et al. (2017) sampled an extensive region of the Barnett Shale footprint (509 groundwater wells covering 14,500 km²) to assess the extent of this spatial cluster and to evaluate likely sources of the stray natural gas. The cluster of groundwater wells with elevated dissolved methane concentrations is located near the Parker and Hood County line, and these wells have high concentrations of dissolved methane and lower than expected concentrations of nitrogen, ²⁰Ne, ³⁶Ar, and ⁸⁴Kr for atmosphere-equilibrated groundwater (Darrah et al., 2014). From this same cluster of groundwater wells Wen et al. (2016) report a positive correlation between dissolved methane and ⁴He, ²¹Ne, and ⁴⁰Ar concentrations, noble gas isotopes which are enriched in the crust relative to the atmosphere (Ballentine et al., 2002). Citing a poor correlation between chloride and dissolved methane in groundwater wells, Darrah et al. (2014) suggest that thermogenic hydrocarbon gas migration was not accompanied by brine and therefore not transported within an aqueous phase. Rather, thermogenic gas in the shallow groundwater was likely transported as a free-gas phase. Wen et al. (2016) directly compare ⁴He/²⁰Ne ratios of dissolved gas in groundwater samples to natural gas samples collected

from the Strawn Group and concludes that stray gas in these water wells is most likely sourced from the Strawn Group, a conclusion that was also reached by Darrah et al. (2014). Although these studies agree on the source of the thermogenic methane, they come to different conclusions on the transport mechanism of natural gas from the Strawn Group to the shallow groundwater of the Trinity Formation; Darrah et al. (2014) suggest transport along well annulus associated with poor cementing techniques, whereas Wen et al. (2016) suggest transport through natural pathways and hydrologic contacts between the overlying Trinity Aquifer and underlying natural gas reservoirs in the Strawn Group. Nicot et al. (2017) provide geologic context to conclude that the vertical distance from the groundwater well screen to the unconformable contact between the Trinity Formation and the Strawn Group is a more important factor than distance to Barnett Shale and conventional horizontal wells. These observations are used to show that, at least within the Barnett Shale footprint, hydraulic fracturing of the Barnett Shale has not provided the source or transport mechanism for natural gas observed in shallow groundwater (Darrah et al., 2014; Nicot et al., 2017; Wen et al., 2016).

Nitrogen is the most abundant nonhydrocarbon gas associated with natural gas reservoirs (Ballentine et al., 2002; Krooss et al., 1995) with measured concentrations that range from trace to nearly 100% (Ballentine et al., 2002; Jenden et al., 1988; Krooss et al., 1995; Márquez et al., 2013; Mingram et al., 2003). Subsurface sources of nitrogen gas include metamorphic and diagenetic alteration of high ammonium clays, primordial gas from the mantle, denitrification of nitrate, and thermogenic cracking of sedimentary organic matter (Golding et al., 2013; Jenden et al., 1988; Krooss et al., 1995). The dominant source of dissolved nitrogen in shallow groundwater is atmospheric in origin and incorporated during equilibrium dissolution in the near surface ($\delta^{15}\text{N} = +0.7\text{‰}$; Klots & Benson, 1963) and as an excess gas trapped as bubbles of air ($\delta^{15}\text{N} = 0\text{‰}$; Cey et al., 2009; Heaton & Vogel, 1981; Vogel et al., 1981). At groundwater recharge temperatures of 18–20 °C dissolved nitrogen concentrations of 14–15 mg/L are expected for atmospheric saturated water (ASW) based on Henry's law calculations (Weiss, 1970). Unlike noble gases that are unaffected by microbial processes and are inert with respect to reaction with geologic substrate, the nitrogen cycle in groundwater is more complex and additional processes that affect nitrogen must be considered. Foremost, microbial denitrification of nitrate produces nitrogen gas which can affect the dissolved nitrogen concentration and its $\delta^{15}\text{N}$ value (Knowles, 1982). Important to methane studies, stray natural gas will increase the availability of methane and may activate anaerobic oxidation coupled to nitrate (Ettwig et al., 2010; Knowles, 1982) and/or sulfate (Valentine & Reeburgh, 2000) reduction. In reducing groundwater systems, denitrification of nitrate to nitrogen is thermodynamically favored over sulfate reduction (Stumm & Morgan, 2012), and in both instances the oxidized by-product of methane is CO_2 in the form of DIC. Studies addressing dissolved nitrogen must therefore account for dissolved nitrogen, methane, and inorganic carbonate species.

This study tests the hypothesis that dissolved nitrogen chemistry may provide an additional means to distinguish sources of stray gas and help differentiate regions with high and low flux of stray gas. This hypothesis is based on stray gas having a nitrogen concentration that is lower than atmospheric, and a nitrogen isotope value that is distinct from atmospheric such that the residual reservoir of dissolved nitrogen in the groundwater phase will be lower than expected for ASW (i.e., *stripping* of dissolved nitrogen) and isotopically distinct (i.e., *isotope exchange*). In this study we use dissolved gas chemistry from samples collected within the Barnett Shale footprint. Measured concentrations of dissolved methane are used as a primary means to identify groundwater wells that are potentially affected by stray gas. Dissolved alkane chemistry is used to attribute methane to either microbial or thermogenic sources. Mixing models based on the relationships presented by Ballentine et al. (2002) are constructed for dissolved nitrogen concentration and its $\delta^{15}\text{N}$ value with consideration given to the addition of dissolved nitrogen through anaerobic methane oxidation. This research builds off published observations and conclusions (Darrah et al., 2014; Wen et al., 2016, 2017) for shallow groundwater wells in the Barnett Shale footprint. Comparing dissolved nitrogen chemistry results reported here with dissolved noble gas ratios measured from the same wells (Wen et al., 2016) and from the same geographic cluster of wells as reported by Darrah et al. (2014) provides a unique means to test our hypothesis. We specifically chose the nitrogen system to develop gas mixing models rather than using the alkane system alone because of the contrasting sensitivity to change between these systems. Whereas the migration of small volumes of stray natural gas into ASW will have large effects on observed dissolved methane concentrations, larger volumes of natural gas are required to change the dissolved nitrogen concentration of ASW, and even

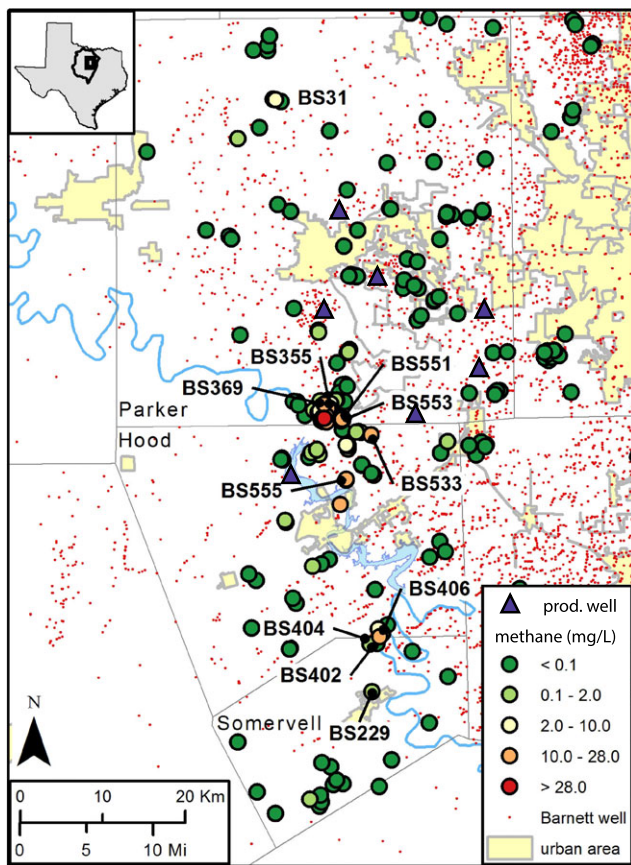


Figure 1. Field map showing groundwater well locations (circles) and Barnett Shale natural gas production wells (small red dots). Purple triangles are producing wells that were sampled in this study. Colors of the circles correspond to concentration of dissolved methane and are grouped using the classification described in the text for trace, low, intermediate, high, and elevated concentrations. Parker and Hood county lines are shown, and urban areas associated with the Dallas Fort Worth metroplex are highlighted in yellow.

more volumes are required to change the $\delta^{15}\text{N}$ value of ASW. Therefore, nitrogen, along with noble gas ratios, may provide an important means to estimate the amount of stray natural gas that has infiltrated into a shallow groundwater aquifer.

2. Study Area

The study area is within Parker and Hood Counties in North Central Texas, just west of the Dallas-Fort Worth Metroplex (Figure 1). Depths to the top of the Barnett Shale approach 1,600 to 1,700 m near the Parker-Hood County line (Pollastro et al., 2007). The Barnett Shale is Mississippian in age and is the target formation for unconventional natural gas hydraulic fracturing with over 20,000 natural gas production wells drilled as of 2015 (IHS, 2015; Jarvie et al., 2007; Pollastro et al., 2007). Natural gas within the Barnett Shale is thermogenic in origin (Montgomery et al., 2005) and is the primary source of natural gas and oil in the Fort Worth Basin, supplying conventional reservoirs within the Ellenburger of Ordovician age, the Marble Falls and the Strawn of Pennsylvanian age, and other rock units (Jarvie et al., 2007; Loucks & Ruppel, 2007; Montgomery et al., 2005). Syn-depositional and postdepositional burial depths were sufficient to reach oil- and gas-generation stages, and within the study area the Barnett Shale generated significant volumes of natural gas through multistage thermal cracking of kerogen, bitumen, and oil (Jarvie et al., 2007; Montgomery et al., 2005; Pollastro et al., 2007). Transport of natural gas from the Barnett Shale into surrounding reservoirs likely occurred during gas-generation stages as increased thermal maturity resulted in pressure increases and microfracturing, thereby creating pathways for subsurface fluid migration (Jarvie et al., 2007; Wen et al., 2017). The Barnett Shale is unconformably overlain by the Pennsylvanian-aged Marble Falls Limestone, which is a massive limestone unit. Above the Marble Falls Limestone, and of primary importance to this study, is the Pennsylvanian-aged Strawn Group which consists of fluvial-deltaic sandstone facies that have trapped migrating oil and gas from source rocks that may include the underlying Mississippian Barnett Shale, coeval organic-rich Pennsylvanian rocks, or the Late Devonian Woodford shale (Ball & Perry, 1995; Brown, 1973). The isolated and discontinuous nature of natural gas pockets within the Strawn Group have made it a difficult reservoir to target for natural gas production; however, its potential as a natural reservoir has been explored since the 1930s.

Unconformably above the Strawn Group in the study area lies early Cretaceous sandstone, basal conglomerates, and interbedded clays that are referred to as the Trinity Group. The Trinity Group hosts the Trinity aquifer, which is the primary fresh water source for the study area (Ashworth et al., 1995; Chaudhuri & Ale, 2013) and the primary aquifer from which groundwater samples were collected in this study. The unconformable contact between the underlying Strawn Group and the Trinity Group does provide for a hydrologic connectivity. Recharge to the Trinity Aquifer occurs through precipitation on exposed outcrop and downward seepage from rivers. Recharge rates within the Trinity Aquifer between 2 and 3 cm/year are reported (Nordstrom, 1982); however, this is an average for a large region and may not be representative of recharge rates within the field area.

3. Methods

3.1. Groundwater Collection

Groundwater samples were collected from residential, irrigation, and municipal groundwater wells between December 2013 and January 2015 with a specific focus on Parker and Hood Counties (Figure 1). Samples collected for dissolved gases, dissolved inorganic carbon, sulfate, and nitrate were collected at the same time at each well. Noble gas data from Wen et al. (2016) that are discussed in this paper were also collected at the

same time. Sample locations cover a wide geographical area that has seen considerable activity from hydraulic fracturing operations (Nicot et al., 2014). Groundwater wells in this area (depths < 250 m) are typically sourced in the lower Cretaceous Trinity aquifer system (Nicot, 2013; Nicot et al., 2014). However, some groundwater wells penetrate the unconformably underlying Strawn Group. Water samples were collected for dissolved methane, ethane, propane, and nitrogen concentration and stable isotope measurements. Additional water samples were collected to measure DIC concentrations and carbon isotope measurements, and sulfate and nitrate concentrations. Specific requirements were followed to obtain representative groundwater samples. We ensured that sampled groundwater wells were (1) drilled to shallow groundwater aquifers and (2) did not contain any type of storage reservoir or filtration device.

Groundwater wells were allowed to flow for at least 15 min to purge standing water, remove any pockets of air that may have accumulated through time, and until pH, temperature, and oxidation reduction potential (ORP) stabilized. Water samples for dissolved gas analysis were collected using a flow-through serum bottle sampling technique with 80-ml glass serum vials capped with 20-mm blue chlorobutylm septa (Bellco part number 2,048–11,800) and crimped with an aluminum seal. The vials are septa sealed prior to filling with water, and two syringes (one fill and one back-vent syringe) are used to fill the vial with groundwater using a small length of clear tubing. At least five vial volumes of water are flushed through the vial. This procedure of precapping, filling, and flushing the vials is essential to ensure that dissolved gas is not lost during sampling, residual gas bubbles are purged, and to minimize the potential for atmospheric contamination. This flow-through sampling technique also has the added benefit that excess dissolved gas (i.e., gas bubbles formed in the groundwater well) is not collected. Water samples collected in the serum bottles are stored at 4 °C and acidified with 0.1 ml of 12-M hydrochloric acid. Groundwater samples for DIC measurement were filtered with a 0.2 micron filter, collected in 40-ml amber vials without headspace, and refrigerated until analysis.

3.2. Groundwater Analysis

Dissolved gas concentrations and carbon isotope values are measured for each sample using a headspace equilibration technique (Kampbell & Vandegrift, 1998). A headspace of pure helium is created in the serum vial by simultaneously injecting 5 ml of pure helium while removing 5 ml of water using two Hamilton Gastight series 1000 headspace syringes. Once completed both syringes are simultaneously removed and the serum bottle is preserved for subsequent analysis. To screen all samples, 4 ml of the removed water is immediately injected into a 6-ml Labco Exetainer[®] headspace vial that was prepurged with helium and evacuated. Adding this volume of water to the Exetainer[®] in no way affects the integrity of the sample in the serum vial, but allows us to automatically screen a large number of samples for dissolved methane concentration. Samples without detectable concentrations of methane are not reanalyzed routinely (however, a subset of nondetect samples were reanalyzed for assurance purposes), whereas samples with detectable methane are reanalyzed directly from the serum bottle using a manually operated syringe. The automated screening technique is simply a means to identify samples that are free of methane, which are not reanalyzed using the more labor intensive manual serum bottle analysis technique.

Concentrations of alkanes (C1 through C3) are measured using an Agilent 7890 gas chromatograph optimized for natural gas with a poraplot Q column and a flame ionization detector. A series of six internal methane gas standards that range from 200 ppb to 7.5%, Scott Gas natural gas standard (TNB00060-14) for methane (88.73%), ethane (3.5%), and propane (1.0%), and Scott Gas natural gas mixture for methane (100 ppm), ethane (100 ppm), and propane (100 ppm) were used for calibration. Exactly 225 μ L of headspace gas is injected, yielding an analytical detection limit of approximately 500 ppb for methane, ethane, and propane. Measured headspace concentrations of methane, ethane, propane, and nitrogen are used to calculate dissolved gas concentrations (Kampbell & Vandegrift, 1998). These calculations account for the volume of liquid and gas headspace in the serum bottle, temperature, and Henry's Law constants for each gas species. Detection limits of at least 0.001 mg/L for methane (C1), 0.002 mg/L for ethane (C2), and 0.003 mg/L for propane (C3) are achieved (Kampbell & Vandegrift, 1998). Less than 0.5% analytical error is routinely achieved on standard reference gases. Replicate analyses of dissolved gas samples, which combine errors associated with sample preparation and analysis were less than 4%. In terms of error of dissolved methane concentration, a 4% total error correlates to an uncertainty of ± 0.05 mg/L for a sample with a 1.0-mg/L concentration of dissolved methane and ± 0.5 mg/L for a sample with 8.0-mg/L dissolved methane, for example.

Table 1

Alkane and Nitrogen Gas Chemistry Measured From Natural Gas Production Wells Sourced in the Barnett Shale and Strawn Group

| Sample | Source | County | Latitude | Longitude | Methane | Ethane | Propane | $\delta^{13}\text{C}$ methane | N2% | $\delta^{15}\text{N}$ N ₂ | Source |
|-----------|---------------|--------|----------|-----------|---------|--------|---------|-------------------------------|-----|--------------------------------------|----------------------|
| BG-5 | Barnett Shale | Hood | 32.51 | -97.84 | 75.1 | 14.4 | 5.4 | -48 | 1.4 | -4.2 | This study |
| BG-6 | Barnett Shale | Parker | 32.66 | -97.81 | 75.3 | 14.4 | 5.3 | -48.7 | 0.9 | -6.1 | This study |
| BG-4 | Barnett Shale | Parker | 32.67 | -97.8 | 76.5 | 13.8 | 5 | -48.6 | 0.7 | -7.7 | This study |
| BG-9 | Barnett Shale | Parker | | | 77.2 | 13.5 | 4.6 | -47.2 | 0.9 | -4.1 | This study |
| BG-1 | Barnett Shale | Parker | 32.7 | -97.79 | 77.5 | 13.3 | 4.8 | -47.9 | 0.9 | -5.69 | This study |
| BG-2 | Barnett Shale | Parker | 32.7 | -97.79 | 77.6 | 13 | 4.7 | -47.6 | 0.9 | -5 | This study |
| BG-7 | Barnett Shale | Parker | 32.72 | -97.63 | 79.4 | 12.6 | 4 | -44.5 | 0.7 | -2.4 | This study |
| BG-8 | Barnett Shale | Parker | 32.72 | -97.63 | 79.7 | 12.4 | 3.9 | -44.1 | 0.7 | -1.8 | This study |
| Barnett-1 | Barnett Shale | | | | 78 | 12.2 | | 47.5 | 0.9 | n.a. | Darrah et al. (2014) |
| Barnett-2 | Barnett Shale | | | | 72 | 15.4 | | -47.4 | 1.2 | n.a. | Darrah et al. (2014) |
| BG-3 | Strawn Group | Parker | 32.67 | -97.8 | 82.1 | 8 | 3.9 | -47.4 | 2.7 | -6.5 | This study |
| Strawn-1 | Strawn Group | | | | 83 | 7.9 | n.a. | -47.9 | 5.6 | n.a. | Darrah et al. (2014) |
| Strawn-2 | Strawn Group | | | | 84 | 6.9 | n.a. | -47.6 | 4.6 | n.a. | Darrah et al. (2014) |
| Strawn-3 | Strawn Group | | | | 85 | 8 | n.a. | -48.6 | 3.3 | n.a. | Darrah et al. (2014) |
| Strawn-4 | Strawn Group | | | | 84 | 9.1 | n.a. | -47.6 | 3.5 | n.a. | Darrah et al. (2014) |

Note. Concentration is reported in percent and isotope values are reported in standard permil notation. Abbreviations: n.a. = not analyzed.

Dissolved nitrogen concentrations and nitrogen isotope values were measured using a 225- μL injection of headspace gas that was also used to measure carbon isotopes of methane. Here we used an Agilent 7890 GC with a 5-mol sieve column and a nondestructive thermal conductivity detector (TCD). This method provided excellent separation of nitrogen, oxygen, and methane, which is critical for accurate methane carbon isotope analysis; any tailing of the nitrogen peak over the methane peak may cause errors during carbon isotope measurement due to formation of N₂O in the ion source, the degree of which will depend on the relative concentrations of methane and nitrogen. Nitrogen concentrations were measured using peak areas collected on the TCD and were calibrated against a series of five internally developed nitrogen standards and a 2.5% nitrogen in natural gas standard (Supelco cat. no. 303101). Methane is combusted to CO₂ using a narrow-bore quartz glass reactor heated to 700 °C packed with copper oxide and analyzed for its $\delta^{13}\text{C}$ value using a Thermo Fisher Scientific Delta V Isotope Ratio Mass Spectrometer directly coupled to the GC-TCD through a Conflo IV peripheral. Carbon isotopes are calibrated against measurements of three internal methane standards ($\delta^{13}\text{C} = -52.8, -39.8, \text{ and } -95.5\text{‰}$) that are calibrated with respect to NBS-19 having a $\delta^{13}\text{C}_{\text{VPDB}}$ equal to +1.95‰. The $\delta^{13}\text{C}$ value of these three internally developed methane standards were verified by sending aliquots of gas for measurement at Isotech® Laboratories. Dissolved nitrogen isotope values are measured directly on N₂ gas using a Thermo Fisher Scientific Delta V Isotope Ratio Mass Spectrometer directly coupled to the GC-TCD through a Conflo IV peripheral. Nitrogen isotope values are reported with respect to $\delta^{15}\text{N}_{\text{AIR}} = 0\text{‰}$ using an air reference gas and a natural gas standard with 2.5% nitrogen. Replicate analyses of dissolved methane samples resulted in a standard deviation of $\pm 0.35\%$ for $\delta^{13}\text{C}$ for methane and $\pm 0.4\%$ for $\delta^{15}\text{N}$ for nitrogen.

DIC concentrations and carbon isotope values were measured using a Thermo Electron Gas Bench II coupled to a Thermo Electron MAT 253 Isotope Ratio Mass Spectrometer (Torres et al., 2005; Waldron et al., 2014). All DIC $\delta^{13}\text{C}$ values are reported relative to NBS-19 having a $\delta^{13}\text{C}_{\text{PDB}}$ equal to +1.95‰ with a standard deviation of $\pm 0.15\%$. DIC concentrations were calculated using a series of six internal calibration standards that cover the range of concentration measured. An error of less than 3% was achieved for all concentration measurements.

4. Results

4.1. Produced Gas Chemistry

Samples of natural gas were collected from nine producing wells (eight from the Barnett Shale and one from the Strawn Group) and analyzed for their natural gas chemistry. Locations of the sampled producing wells are illustrated in Figure 1. We include published data from Darrah et al. (2014) for Strawn and Barnett production wells in addition to production wells collected in this study. Alkane and nitrogen concentrations and the stable carbon isotope ratios of methane and nitrogen are listed in Table 1. Gas dryness (C1/C2 + C3

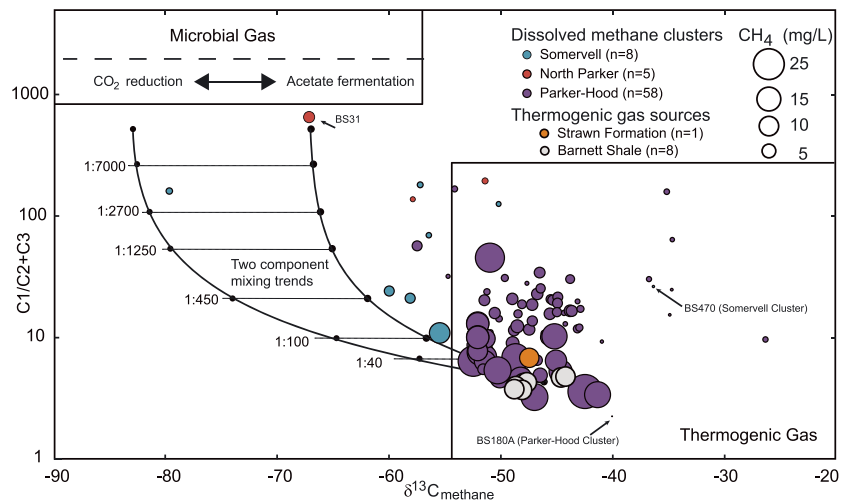


Figure 2. Bernard plot (Bernard et al., 1977) showing carbon isotope values and gas dryness for sampled wells. Circle size correlates to concentration of dissolved methane. Samples are grouped into the three clusters described in the text. Sources of produced gas from Barnett Shale and Strawn Group are also shown. Two-component mixing lines between Barnett Shale produced natural gas, and two different microbial end member sources are illustrated along with calculated volumetric gas:water mixing ratios.

alkane ratios) is plotted with respect to carbon isotope values of methane in Figure 2. Gas dryness averages $4.5 \pm 0.8\%$ ($n = 10$) for the Barnett Shale and $9.9 \pm 2.0\%$ ($n = 5$) for the Strawn Group. Carbon isotope values of methane from the Barnett Shale and the Strawn Group are indistinguishable at $-47.2 \pm 1.6\text{‰}$ and $-47.8 \pm 0.5\text{‰}$, respectively. These values are consistent with those reported by Rodriguez and Philp (2010) for samples collected in Parker county. Nitrogen molar concentrations of $0.9 \pm 0.2\%$ ($n = 10$) and $\delta^{15}\text{N}$ values that range from -1.8 to -7‰ ($n = 8$) are measured for the Barnett Shale samples (Table 1). One sample measured in this study area from the Strawn Group has a $\delta^{15}\text{N}$ value of -6.5‰ , and five samples from the Strawn Group have nitrogen molar concentrations that range from 2.7% to 5.6% (average = $3.94 \pm 1.2\%$, Table 1). Nitrogen concentrations measured in this study are consistent with published nitrogen concentrations of $1.05 \pm 0.2\%$ ($n = 2$) and $4.25 \pm 1.1\%$ ($n = 4$) measured from the Barnett Shale and Strawn Group, respectively (Darrah et al., 2014; Table 1). In the following sections we develop a model to compare the effects of mixing groundwater water with low- and high-nitrogen natural gas representative of nitrogen concentrations measured from the Strawn Group and Barnett Shale and discuss the effect that nitrogen content may have on resulting groundwater-dissolved nitrogen isotope values (Kornacki & McCaffrey, 2014; Kreitler & Browning, 1983).

4.2. Spatial Distribution of Dissolved Methane

Dissolved methane concentrations measured from 457 wells in Parker, Hood, Somervell, and surrounding counties are illustrated in Figure 1. These data are reported in Table S2 of Nicot et al. (2017). Locations of hydraulic fracturing wells within these counties are also illustrated. Dissolved methane concentrations are grouped using a modified classification system outlined by the U.S. Department of the Interior Office of Surface Mining (Elt Schlager et al., 2001): <0.1 mg/L *trace*; 0.1 to 2 mg/L *low*; 2–10 mg/L *intermediate*; 10–28 mg/L *high*; and >28 mg/L *elevated*. Using this classification, 424 out of 457 groundwater wells analyzed in this study yielded trace to low concentrations of dissolved methane (Nicot et al., 2017). Three clusters of samples with intermediate, high, and elevated dissolved methane concentrations are identified (Figure 1). The largest cluster is located at the border of Parker and Hood counties (referred to as the *Parker-Hood cluster*). Two smaller clusters are observed to the north *North Parker cluster* and south *Somervell cluster* of the Parker-Hood cluster. Additional groundwater wells from the Parker-Hood cluster were obtained to better delineate the spatial extent of this cluster. Here we focus on samples collected within and near the described clusters that come from 77 unique groundwater wells for a total number of 118 samples with replicates. Comparison of dissolved methane concentrations from groundwater wells that were visited and sampled multiple times are in good agreement. More variability is observed for higher concentration samples compared to wells with low to trace concentrations of dissolved methane. For example, methane concentrations from repeat sampling of well BS200 are 24.5 and 18.3 mg/L, and 14.6 and 18.0 mg/L for well BS358. This observed variability with higher

Table 2
Dissolved Alkane and Nitrogen Chemistry Measured From Shallow Groundwater Wells in the Field Area

| Sample ID | Cluster | Lat | Long | Depth (ft) | Methane (mg/L) | Ethane (mg/L) | Propane (mg/L) | Gas wetness | $\delta^{13}\text{C}_{\text{CH}_4}$ (‰) | N_2 (mg/L) | $\delta^{15}\text{N}$ (‰) |
|-----------|--------------|-------|--------|------------|----------------|---------------|----------------|-------------|---|---------------------|---------------------------|
| BS029 | North Parker | 32.87 | -97.89 | 180 | 1 | <0.002 | <0.003 | 200 | -51.3 | | |
| BS029B | North Parker | 32.87 | -97.89 | 180 | 0.7 | <0.002 | <0.003 | 140 | -57.8 | | |
| BS031 | North Parker | 32.91 | -97.84 | 170 | 3.4 | <0.002 | <0.003 | 680 | -67.1 | | |
| BS031B | North Parker | 32.91 | -97.84 | 170 | 2 | <0.002 | <0.003 | 400 | -67.2 | | |
| BS031C | North Parker | 32.91 | -97.84 | 170 | 2.1 | <0.002 | <0.003 | 420 | -62.1 | 10.4 | 0.8 |
| BS168 | Outside | 32.63 | -97.75 | 400 | 0.1 | <0.002 | <0.003 | 20 | b.d. | 17.5 | 0.7 |
| BS178A | Outside | 32.58 | -97.82 | 110 | 0.1 | <0.002 | <0.003 | 20 | b.d. | 19.8 | 0.7 |
| BS179 | Outside | 32.58 | -97.83 | 80 | <0.001 | <0.002 | <0.003 | n.a. | b.d. | | |
| BS179A | Outside | 32.58 | -97.83 | 80 | <0.001 | <0.002 | <0.003 | n.a. | b.d. | 27.6 | 0.4 |
| BS197 | Outside | 33.06 | -97.6 | 390 | 0.2 | <0.002 | <0.003 | 40 | b.d. | 19 | 0.7 |
| BS207 | Outside | 32.57 | -97.77 | 322 | <0.001 | <0.002 | <0.003 | n.a. | b.d. | | |
| BS207A | Outside | 32.57 | -97.77 | 322 | 0.1 | <0.002 | <0.003 | 20 | b.d. | 20.6 | 0.5 |
| BS229 | Outside | 32.26 | -97.73 | | 0.2 | <0.002 | <0.003 | 40 | b.d. | 13 | 0.6 |
| BS232 | Outside | 32.14 | -97.81 | 400 | 0.1 | <0.002 | <0.003 | 20 | b.d. | 17.6 | 0.4 |
| BS254 | Outside | 32.97 | -97.85 | 180 | <0.001 | <0.002 | <0.003 | n.a. | b.d. | | |
| BS254A | Outside | 32.97 | -97.85 | 180 | <0.001 | <0.002 | <0.003 | n.a. | b.d. | 20.4 | 0.7 |
| BS255 | Outside | 32.96 | -97.87 | 360 | <0.001 | <0.002 | <0.003 | n.a. | b.d. | | |
| BS255A | Outside | 32.96 | -97.87 | 360 | <0.001 | <0.002 | <0.003 | n.a. | b.d. | 19.5 | 0.9 |
| BS311 | Outside | 32.4 | -97.81 | 357 | 0.3 | <0.002 | <0.003 | 60 | b.d. | 16.9 | 0.5 |
| BS338 | Outside | 32.54 | -97.75 | 440 | 0.1 | <0.002 | <0.003 | 20 | b.d. | 14.6 | 0.3 |
| BS338A | Outside | 32.54 | -97.75 | 440 | <0.001 | <0.002 | <0.003 | n.a. | b.d. | 17.8 | 0.2 |
| BS343 | Outside | 32.44 | -97.33 | 100 | 0.2 | <0.002 | <0.003 | 40 | b.d. | 14.3 | 0.5 |
| BS351 | Outside | 32.58 | -97.77 | 345 | <0.001 | <0.002 | <0.003 | n.a. | b.d. | | |
| BS351A | Outside | 32.58 | -97.77 | 345 | 0.1 | <0.002 | <0.003 | 20 | b.d. | 18.6 | 0.4 |
| BS352 | Outside | 32.57 | -97.78 | | 0.3 | <0.002 | <0.003 | 60 | b.d. | 14.9 | 0.6 |
| BS364A | Outside | 32.59 | -97.76 | 325 | <0.001 | <0.002 | <0.003 | n.a. | b.d. | | |
| BS365 | Outside | 32.59 | -97.76 | 375 | <0.001 | <0.002 | <0.003 | n.a. | b.d. | | |
| BS365A | Outside | 32.59 | -97.76 | 375 | <0.001 | <0.002 | <0.003 | n.a. | b.d. | 18.7 | 0.5 |
| BS367A | Outside | 32.6 | -97.76 | <0.001 | <0.002 | <0.003 | n.a. | b.d. | | | |
| BS370 | Outside | 32.52 | -97.8 | 220 | 0.2 | <0.002 | <0.003 | 40 | b.d. | 18.4 | 0.5 |
| BS446 | Outside | 32.58 | -97.77 | 100 | <0.001 | <0.002 | <0.003 | n.a. | b.d. | | |
| BS446A | Outside | 32.58 | -97.77 | 100 | <0.001 | <0.002 | <0.003 | n.a. | b.d. | 20.8 | 0.4 |
| BS534 | Outside | 32.46 | -97.77 | 275 | <0.001 | <0.002 | <0.003 | n.a. | b.d. | | |
| BS534B | Outside | 32.46 | -97.77 | 275 | <0.001 | <0.002 | <0.003 | n.a. | b.d. | | |
| BS534C | Outside | 32.46 | -97.77 | 275 | <0.001 | <0.002 | <0.003 | n.a. | b.d. | 11.6 | 0.4 |
| BS554 | Outside | 32.56 | -97.77 | 320 | 0.8 | <0.002 | <0.003 | 160 | b.d. | 23.1 | 0.4 |
| BS016B | Parker-Hood | 32.57 | -97.8 | 150 | 0.7 | <0.002 | <0.003 | 140 | -44.3 | | |
| BS016C | Parker-Hood | 32.57 | -97.8 | 150 | 0.6 | <0.002 | <0.003 | 120 | -48.8 | 22.1 | 0.7 |
| BS017 | Parker-Hood | 32.57 | -97.79 | 175 | <0.001 | <0.002 | <0.003 | n.a. | b.d. | | |
| BS017B | Parker-Hood | 32.57 | -97.79 | 175 | 0.2 | <0.002 | <0.003 | 40 | 34.6 | | |
| BS017C | Parker-Hood | 32.57 | -97.79 | 175 | <0.001 | <0.002 | <0.003 | n.a. | b.d. | | |
| BS112A | Parker-Hood | 32.57 | -97.8 | | 0.7 | 0.1 | <0.003 | 7 | -26.2 | 20 | 0.7 |

Table 2 (continued)

| Sample ID | Cluster | Lat | Long | Depth (ft) | Methane (mg/L) | Ethane (mg/L) | Propane (mg/L) | Gas wetness | $\delta^{13}\text{C}_{\text{CH}_4}$ (‰) | N_2 (mg/L) | $\delta^{15}\text{N}$ (‰) |
|-----------|-------------|-------|--------|------------|----------------|---------------|----------------|-------------|---|---------------------|---------------------------|
| BS175 | Parker-Hood | 32.65 | -97.79 | 285 | 0.4 | <0.002 | <0.003 | 80 | -54.7 | 13.5 | 0.5 |
| BS180 | Parker-Hood | 32.58 | -97.82 | 320 | <0.001 | <0.002 | <0.003 | n.a. | b.d. | | |
| BS180A | Parker-Hood | 32.58 | -97.82 | 320 | <0.001 | <0.002 | <0.003 | n.a. | -40 | 19.4 | 0.8 |
| BS199 | Parker-Hood | 32.56 | -97.79 | 180 | 31 | 6.2 | 2.2 | 4 | -42.4 | | |
| BS199B | Parker-Hood | 32.56 | -97.79 | 180 | 19.2 | 4.3 | 1.6 | 3 | -46.9 | | |
| BS200 | Parker-Hood | 32.55 | -97.78 | 368 | 24.5 | 3.7 | <0.003 | 7 | -52.4 | | |
| BS200B | Parker-Hood | 32.55 | -97.78 | 368 | 18.3 | 2.3 | <0.003 | 8 | -51.8 | | |
| BS201 | Parker-Hood | 32.56 | -97.77 | 470 | 5.4 | 0.9 | 0.2 | 5 | -46.4 | | |
| BS201B | Parker-Hood | 32.56 | -97.77 | 470 | 5.4 | 0.9 | 0.2 | 5 | -48 | | |
| BS201C | Parker-Hood | 32.56 | -97.77 | 470 | 5.1 | 0.9 | 0.2 | 5 | -49.7 | | |
| BS202 | Parker-Hood | 32.56 | -97.78 | 186 | 14.1 | 2.1 | 0.6 | 5 | -44.6 | | |
| BS204 | Parker-Hood | 32.56 | -97.79 | 200 | 3.5 | 0.2 | <0.003 | 17 | -43.7 | | |
| BS204B | Parker-Hood | 32.56 | -97.79 | 200 | 3.2 | 0.2 | <0.003 | 16 | -43.6 | | |
| BS204C | Parker-Hood | 32.56 | -97.79 | 200 | 3.5 | 0.2 | <0.003 | 17 | -45.5 | | |
| BS205 | Parker-Hood | 32.56 | -97.79 | 200 | 4.3 | 0.5 | <0.003 | 9 | -48.9 | | |
| BS206 | Parker-Hood | 32.58 | -97.77 | | 0.6 | <0.002 | <0.003 | 120 | -50.8 | | |
| BS208 | Parker-Hood | 32.56 | -97.79 | 210 | 2.1 | 0.1 | <0.003 | 20 | -45.5 | | |
| BS208B | Parker-Hood | 32.56 | -97.79 | 210 | 2.7 | 0.1 | <0.003 | 26 | -45.3 | | |
| BS209 | Parker-Hood | 32.56 | -97.78 | 285 | 2.6 | 0.1 | <0.003 | 25 | -44.8 | | |
| BS209B | Parker-Hood | 32.56 | -97.78 | 285 | 2.7 | 0.1 | <0.003 | 26 | -44.9 | | |
| BS210 | Parker-Hood | 32.56 | -97.79 | 130 | 0.4 | <0.002 | <0.003 | 80 | -47.6 | 15.8 | 0.5 |
| BS211 | Parker-Hood | 32.57 | -97.78 | 350 | 3.5 | 0.1 | <0.003 | 34 | -48.9 | | |
| BS211B | Parker-Hood | 32.57 | -97.78 | 350 | 3.6 | 0.2 | <0.003 | 18 | -47.1 | | |
| BS211C | Parker-Hood | 32.57 | -97.78 | 350 | 3.4 | 0.1 | <0.003 | 33 | -46.7 | 14.8 | 0.7 |
| BS221 | Parker-Hood | 32.56 | -97.79 | 120 | 2.8 | 0.4 | <0.003 | 7 | -46.7 | | |
| BS222 | Parker-Hood | 32.56 | -97.78 | 183 | 2.3 | 0.1 | <0.003 | 22 | -46.4 | | |
| BS244 | Parker-Hood | 32.45 | -97.84 | | 0.9 | 0.1 | <0.003 | 9 | -51.1 | | |
| BS340 | Parker-Hood | 32.54 | -97.74 | | 1.3 | <0.002 | <0.003 | 260 | -49.6 | | |
| BS340A | Parker-Hood | 32.54 | -97.74 | | 1 | <0.002 | <0.003 | 200 | -51.2 | 15.5 | 0.5 |
| BS347 | Parker-Hood | 32.57 | -97.79 | 240 | 2.3 | 0.1 | <0.003 | 22 | -44.9 | | |
| BS347A | Parker-Hood | 32.57 | -97.79 | 240 | 2.7 | 0.2 | <0.003 | 13 | -47.1 | 18.2 | 1.9 |
| BS348 | Parker-Hood | 32.57 | -97.78 | | 2 | 0.1 | <0.003 | 19 | -48 | | |
| BS348A | Parker-Hood | 32.57 | -97.78 | | 1.8 | 0.1 | <0.003 | 17 | -48.4 | 20.1 | 0.5 |
| BS349 | Parker-Hood | 32.52 | -97.79 | 199 | 0.6 | <0.002 | <0.003 | 120 | -44.2 | | |
| BS353 | Parker-Hood | 32.58 | -97.79 | 270 | 0.6 | <0.002 | <0.003 | 120 | -43.1 | | |
| BS354 | Parker-Hood | 32.58 | -97.77 | 380 | <0.001 | <0.002 | <0.003 | n.a. | b.d. | | |
| BS354A | Parker-Hood | 32.58 | -97.77 | 380 | 0.2 | <0.002 | <0.003 | 40 | -34.8 | 20.9 | 0.6 |
| BS355 | Parker-Hood | 32.57 | -97.78 | 225 | 20.1 | 2.7 | 0.1 | 7 | -48.6 | | |
| BS355A | Parker-Hood | 32.57 | -97.78 | 225 | 12.7 | 1.8 | <0.003 | 7 | -51.3 | 9.4 | 0.4 |
| BS356 | Parker-Hood | 32.56 | -97.79 | | 1.8 | 0.1 | <0.003 | 17 | -43.1 | | |
| BS356A | Parker-Hood | 32.56 | -97.79 | | 1.4 | 0.1 | <0.003 | 14 | -42.9 | 24.5 | 0.6 |
| BS357 | Parker-Hood | 32.57 | -97.79 | 240 | 3.1 | 0.1 | <0.003 | 30 | -46.4 | | |
| BS357A | Parker-Hood | 32.57 | -97.79 | 240 | 2.1 | 0.1 | <0.003 | 20 | -43.7 | 19.4 | -0.1 |
| BS358 | Parker-Hood | 32.57 | -97.78 | 360 | 14.6 | 2.2 | 0.9 | 5 | -48.2 | | |

Table 2 (continued)

| Sample ID | Cluster | Lat | Long | Depth (ft) | Methane (mg/L) | Ethane (mg/L) | Propane (mg/L) | Gas wetness | $\delta^{13}\text{C}_{\text{CH}_4}$ (‰) | N_2 (mg/L) | $\delta^{15}\text{N}$ (‰) |
|-----------|-------------|-------|--------|---------------|-------------------|------------------|-------------------|----------------|--|------------------------|------------------------------|
| BS358A | Parker-Hood | 32.57 | -97.78 | 360 | 18 | 3.5 | 1.7 | 3 | -41.3 | | |
| BS360 | Parker-Hood | 32.58 | -97.78 | 322 | 1.2 | 0.1 | <0.003 | 12 | -46 | | |
| BS361 | Parker-Hood | 32.57 | -97.79 | 210 | 3.3 | 0.3 | <0.003 | 11 | -48.7 | | |
| BS362 | Parker-Hood | 32.56 | -97.79 | 180 | 4.4 | 0.3 | <0.003 | 15 | -48.5 | | |
| BS363 | Parker-Hood | 32.56 | -97.79 | 120 | 1.3 | 0.1 | <0.003 | 13 | -42.8 | | |
| BS369 | Parker-Hood | 32.57 | -97.79 | 300 | 12.1 | 1.7 | 0.2 | 6 | -45 | | |
| BS369A | Parker-Hood | 32.57 | -97.79 | 300 | 11.9 | 1.7 | 0.2 | 6 | -51.4 | 13.4 | 0.2 |
| BS434 | Parker-Hood | 32.57 | -97.79 | | 6 | 0.6 | <0.003 | 10 | -45.7 | | |
| BS434A | Parker-Hood | 32.57 | -97.79 | | 4.8 | 0.5 | 0.1 | 8 | -52.4 | 18.4 | 0.7 |
| BS435 | Parker-Hood | 32.52 | -97.8 | 180 | 0.3 | <0.002 | <0.003 | 60 | -40.9 | | |
| BS436 | Parker-Hood | 32.52 | -97.76 | 320 | 1.1 | 0.1 | <0.003 | 11 | -50.1 | | |
| BS443 | Parker-Hood | 32.53 | -97.76 | 420 | 3.3 | 0.2 | <0.003 | 16 | -50.5 | | |
| BS444 | Parker-Hood | 32.53 | -97.76 | 220 | 3.1 | 0.1 | <0.003 | 30 | -51.4 | | |
| BS447 | Parker-Hood | 32.58 | -97.77 | | 0.5 | <0.002 | <0.003 | 100 | -34.6 | | |
| BS447A | Parker-Hood | 32.58 | -97.77 | | 0.7 | <0.002 | <0.003 | 140 | -36.7 | 20.5 | 0.5 |
| BS448 | Parker-Hood | 32.58 | -97.77 | | 0.8 | <0.002 | <0.003 | 160 | -35.1 | | |
| BS533 | Parker-Hood | 32.54 | -97.73 | 500 | 9.8 | 0.9 | 0.1 | 10 | -51.3 | | |
| BS533B | Parker-Hood | 32.54 | -97.73 | 500 | 13.4 | 1 | <0.003 | 13 | -52 | | |
| BS533C | Parker-Hood | 32.54 | -97.73 | 500 | 17 | 1.6 | 0.1 | 10 | -45.1 | 12.3 | 0 |
| BS544 | Parker-Hood | 32.49 | -97.76 | 420 | 2.6 | <0.002 | <0.003 | 520 | -57.4 | | |
| BS544A | Parker-Hood | 32.49 | -97.76 | 420 | 0.9 | <0.002 | <0.003 | 180 | -54.1 | 16.1 | 0.2 |
| BS551 | Parker-Hood | 32.56 | -97.76 | 363 | 10.3 | 1.8 | 0.3 | 5 | -50 | 6.7 | -0.4 |
| BS552 | Parker-Hood | 32.56 | -97.76 | 385 | 3 | 0.4 | 0.1 | 6 | -51.5 | | |
| BS553 | Parker-Hood | 32.56 | -97.76 | | 19.4 | 2.8 | 0.7 | 6 | -50.2 | 7.2 | -1.1 |
| BS555 | Parker-Hood | 32.49 | -97.76 | 310 | 22.7 | 0.4 | 0.1 | 45 | -50.9 | 8.2 | -2.4 |
| BS237 | Somervell | 32.31 | -97.73 | 1350 | 0.6 | <0.002 | <0.003 | 120 | -510.1 | 17.6 | 0.7 |
| BS307 | Somervell | 32.32 | -97.72 | 425 | 11.3 | 0.8 | 0.2 | 11 | -55.4 | | |
| BS402 | Somervell | 32.32 | -97.72 | 186 | 1.1 | <0.002 | <0.003 | 220 | -79.6 | | |
| BS403 | Somervell | 32.33 | -97.72 | 380 | 2.7 | 0.1 | <0.003 | 26 | -58.1 | | |
| BS404 | Somervell | 32.32 | -97.72 | 370 | 0.8 | 0 | <0.003 | 267 | -56.4 | | |
| BS405 | Somervell | 32.33 | -97.72 | 500 | 2.7 | 0.1 | <0.003 | 26 | -59.9 | | |
| BS406 | Somervell | 32.32 | -97.72 | 395 | 0.9 | <0.002 | <0.003 | 180 | -57.1 | | |

Note. Abbreviations: n.a. = not applicable due to below detection concentrations; b.d. = below detection.

concentration samples (i.e., >20 mg/L) is consistent with sampling effects observed by Molofsky et al. (2016) for wells with high concentrations of dissolved methane and subsequent two-phase systems.

4.3. Dissolved Alkane Chemistry

Methane, ethane, and propane concentrations, corresponding $\delta^{13}\text{C}_{\text{methane}}$ values, and gas dryness ($\text{C}_1/(\text{C}_2 + \text{C}_3)$ alkane ratios) are listed in Table 2. Gas dryness is plotted with respect to carbon isotope values of dissolved methane in Figure 2. Minimum concentration of methane for $\delta^{13}\text{C}_{\text{methane}}$ analysis is approximately 0.1 mg/L (compared to analytical detection limits of 0.001 mg/L for methane concentration); however, most samples plotted have concentrations greater than 0.5 mg/L. Therefore, these data represent a subset ($n = 84$) of samples collected in the field area, with most samples coming from the North Parker, Parker-Hood, and Somervell clusters. The North Parker cluster (five samples from two groundwater wells) contain low to intermediate methane concentrations (0.70 to 3.40 mg/L). Samples from the North Parker cluster preserve alkane chemistry results that are more similar to a microbial methane signature compared to other samples measured in this study. For example, groundwater well BS031 ($n = 3$) has methane concentrations between 3.4 and 2.0 mg/L, nondetect concentrations of ethane and propane, and $\delta^{13}\text{C}_{\text{methane}}$ values between -62

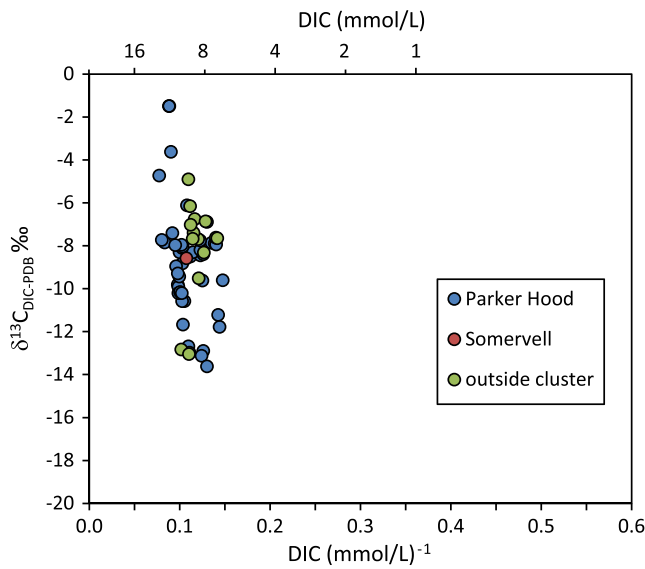


Figure 3. Plot of carbon isotope values of DIC compared to DIC concentration⁻¹ for samples from the Park Hood and Somervell clusters, and outside the clusters. DIC = dissolved inorganic carbon.

istry closely matches natural gas from the Barnett Shale and Strawn Group. Although groundwater wells BS199 and BS555 contain elevated and high dissolved methane concentrations >20 mg/L with a thermogenic signature that is similar to natural gas from the Barnett Shale and Strawn Formation, a groundwater well within 100 m of BS555 (BS544, well depth 125 m) has a lower dissolved methane concentration of 2.6 mg/L. Methane at BS544 also has a thermogenic signature, but the measured difference in concentration over a short distance demonstrates the heterogeneity and localized nature of elevated dissolved methane concentrations in the Parker-Hood cluster. Six groundwater samples from the Parker-Hood cluster have low dissolved methane concentrations (0.16 to 0.84 mg/L) and methane $\delta^{13}\text{C}_{\text{methane}}$ values that are greater than the rest of the samples ($\delta^{13}\text{C} > -37\text{‰}$). The wide range of carbon isotope values and alkane dryness in the measured groundwater samples relative to the more constrained range of values observed for produced natural gas from the Barnett Shale and Strawn Group is discussed in the following sections.

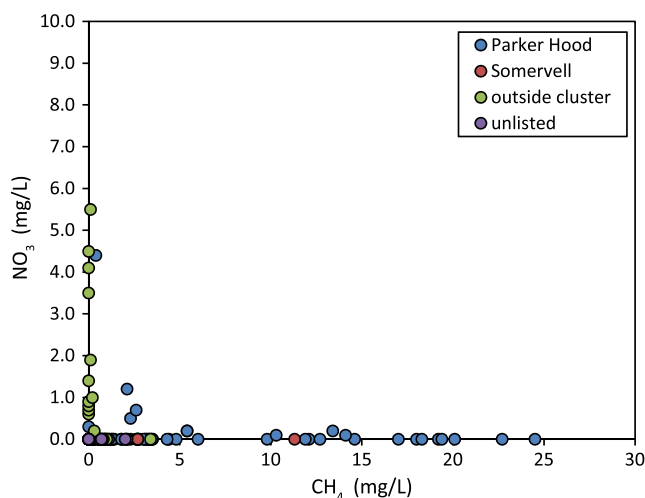


Figure 4. Plot of nitrate concentrations compared to dissolved methane concentrations (mg/L) for samples from the Park Hood and Somervell clusters, and outside the clusters.

and -67‰ (Figure 2). Two samples from groundwater well BS029 have higher $\delta^{13}\text{C}_{\text{methane}}$ values of -57 and -51‰ , but nondetect concentrations of ethane and propane and a lower concentration of dissolved methane 0.7 and 1.0 mg/L. Eight additional samples taken within 10 km of these two groundwater wells have trace (<0.1 mg/L) dissolved methane concentrations pointing to a localized nature for the intermediate dissolved methane concentrations in this area.

Further to the south, the Parker-Hood cluster (Figure 1) is delineated by 47 groundwater wells that encompass an area of approximately 50 km². $\delta^{13}\text{C}_{\text{methane}}$ values for samples from these groundwater wells range between -41 and -52‰ , which is similar to $\delta^{13}\text{C}_{\text{methane}}$ values measured for methane from produced gas from the Barnett Shale and Strawn Group ($\delta^{13}\text{C}$ between -42 and -47‰ ; samples collected in this and other studies, Rodriguez & Philp, 2010). Alkane ratios (C1/(C2 + C3)) range from 3.3 to 22.7, which also closely matches alkane ratios from production wells for the Barnett Shale and Strawn Group collected within 10 km of the Parker-Hood cluster (Figure 2). The majority of the groundwater wells have dissolved methane concentrations above 2 mg/L, with nine groundwater wells having dissolved methane concentrations greater than 10 mg/L, and a maximum dissolved methane concentration of 31 mg/L (BS199) was measured. One groundwater well (BS555, well depth 95 m) has vented natural gas since it was drilled in December 2012. We measured a gas flow rate of 3 L/min at the head of this groundwater well, and its alkane chem-

The Somervell cluster is 25 km to the south of the Parker-Hood cluster (Figure 1). Three different groundwater wells (eight samples) have dissolved methane concentrations that range from 0.64 to 11.3 mg/L. Similar to the Parker-Hood cluster, the highest concentration sample is within 500 m of two groundwater wells with trace concentrations of dissolved methane, further suggesting the localized nature of the clusters defined by high dissolved methane concentration. Samples from the Somervell cluster show the greatest variability of $\delta^{13}\text{C}_{\text{methane}}$ and C1/(C2 + C3) ratios, suggesting thermogenic and microbial methane source mixing (Figure 2). Sample BS402 is unique in this data set in that the dissolved methane has a $\delta^{13}\text{C}$ value of -79.6‰ , suggesting formation from a CO₂ reduction methanogenic pathway (Whiticar, 1999; Wolin & Miller, 1987; Zhang et al., 1998). This is distinct from sample BS031 from the North Parker Cluster, which is also microbial in nature but more consistent with methane acetate methanogenesis.

4.4. Anaerobic Methane Oxidation

Measured concentration and carbon isotope values of DIC range from 6.7 to 13.0 mmol/L with corresponding $\delta^{13}\text{C}$ values that range from -1.5 to -14‰ ($n = 59$) (supplemental Tables S1 and S2 in Nicot et al., 2017). Data for Parker-Hood cluster, Somervell Cluster, and samples

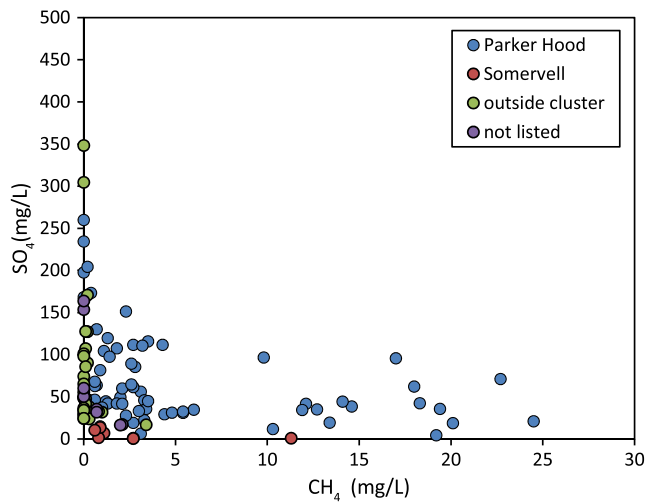


Figure 5. Plot of sulfate concentrations compared to dissolved methane concentrations (mg/L) for samples from the Park Hood and Somervell clusters, and outside the clusters.

Dissolved nitrate and sulfate concentrations for groundwater samples reported by Nicot et al. (2017) are illustrated in Figures 4 and 5, respectively, with respect to dissolved methane concentrations. Groundwater samples collected outside the clusters have nitrate and sulfate concentrations that are higher than observed within the clusters (Figures 4 and 5). Sulfate was detected in all the groundwater samples analyzed, but similar to nitrate, higher concentrations of sulfate were measured outside the Parker-Hood cluster than within (Figure 5). These data suggest anaerobic oxidation of methane coupled to nitrate, and potentially sulfate reduction occurred within the Parker-Hood cluster. Darvari et al. (2017) concluded, based on the distribution

collected outside the clusters are illustrated on a $\delta^{13}\text{C}$ versus DIC^{-1} plot (Figure 3). Anaerobic methane oxidation of stray natural gas results in a negative correlation whereby samples with higher concentrations of DIC have lower $\delta^{13}\text{C}$ values resulting from oxidation of methane with low carbon isotope values ($\delta^{13}\text{C}_{\text{methane}} < -25\text{‰}$ in all samples). The measured data do not follow this trend. Instead, samples with the highest concentration of DIC have the highest $\delta^{13}\text{C}$ value of approximately -3.6‰ , which is more typical of dissolution from marine carbonates. Grossman et al. (1989) observed similar relationships between $\delta^{13}\text{C}$ versus DIC^{-1} from the Sparta aquifer in east Texas, but those groundwater samples contained high concentrations of methane ($>20\text{ mg/L}$) with $\delta^{13}\text{C}$ values that ranged from -58.4 to -53.1‰ , and very low concentrations of coexisting ethane and propane. In their study, Grossman et al. (1989) suggest that a combination of carbonate dissolution, acetate, and CO_2 reduction methanogenesis, and anaerobic oxidation left the residual bicarbonate pool enriched in carbon-13. In this study, the methane in the Parker-Hood cluster is thermogenic in origin, but the trend of $\delta^{13}\text{C}$ versus DIC^{-1} suggests that anaerobic methane oxidation does not contribute significantly to the mass balance of bicarbonate in these waters, or is coupled to CO_2 reduction methanogenesis in such a way to offset the overall effects.

of trace elements in groundwater samples within the Barnett shale footprint, that anaerobic reduction of methane in the nitrate and iron stage did occur with carbonate precipitation. It is uncertain, however, how much groundwater nitrate may have existed prior to nitrate reduction, and therefore, the contribution of nitrate reduction to dissolved nitrogen gas is unknown. Considering that the DIC data (section 4.3) do not support significant methane oxidation, it does not appear that the alkane chemistry could have been significantly affected by subsequent anaerobic methane oxidation. In the context of applying dissolved nitrogen chemistry to attribute sources of methane and estimate source mixing ratios, however, we must consider the effect that any anaerobic oxidation of methane coupled to nitrate reduction could have on the preserved dissolved nitrogen chemistry. In the following section the dissolved nitrogen chemistry of these samples is described, and effects associated with anaerobic oxidation of methane coupled to nitrate reduction is discussed.

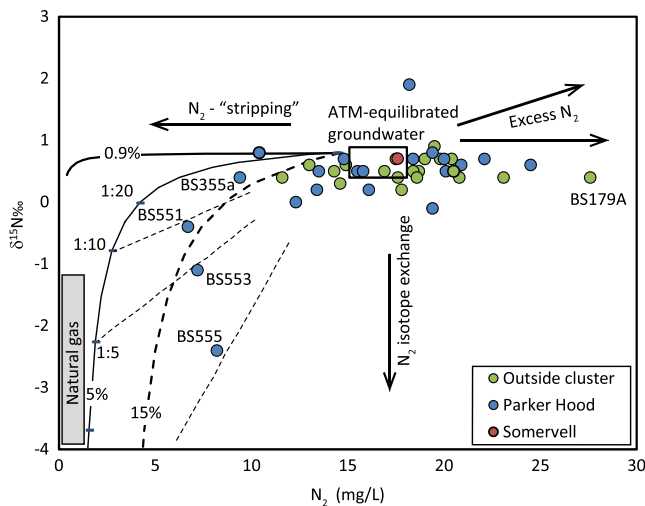


Figure 6. Comparison of dissolved nitrogen $\delta^{15}\text{N}$ values and corresponding concentrations for samples collected within and near the three groundwater well clusters. Trends expected for (1) excess nitrogen, (2) stripped nitrogen, and (3) nitrogen isotope exchange between thermogenic and atmospheric nitrogen are illustrated. Solid lines labeled 0.9% and 5% represent mixing model trends for stray gas from Barnett Shale and Strawn Group, respectively. Bold dashed line shows mixing effects for a hypothetical natural gas with 15% nitrogen. Thin dashed lines show mixing between atmospheric and stripped groundwater reservoirs. Volumetric gas:water mixing ratios (calculated at standard temperature and pressure) are illustrated.

4.5. Dissolved Nitrogen Chemistry

Dissolved nitrogen concentrations and $\delta^{15}\text{N}$ values are measured at 43 locations within Parker-Hood cluster ($n = 21$), the Somervell cluster ($n = 1$), the North Parker cluster ($n = 1$), and outside the clusters ($n = 20$) (Table 2). Samples cover a range of dissolved methane concentrations from nondetect to high and elevated. Dissolved nitrogen concentrations and corresponding $\delta^{15}\text{N}$ values are listed in Table 2. Nitrogen isotope values are plotted relative to dissolved nitrogen concentration in Figure 6. Samples collected outside the Parker-Hood cluster have $\delta^{15}\text{N}$ values that average $0.52 \pm 0.16\text{‰}$ and dissolved nitrogen concentrations that range from 11.6 to 27.6 mg/L. The mean annual air temperature for Granbury, TX, the nearest city to the field area, is 18 °C. Mean annual air temperature is used as

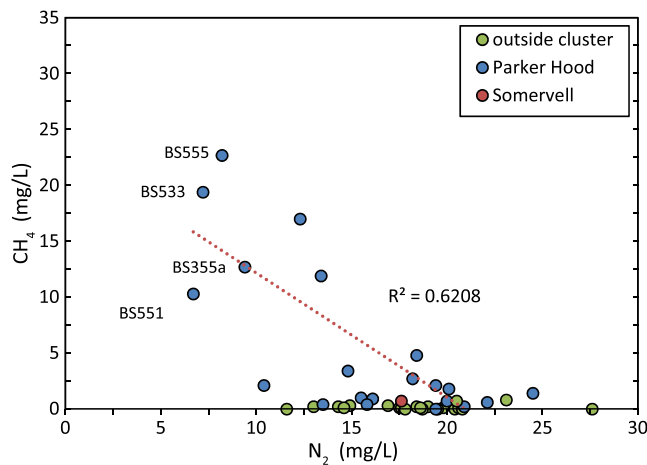


Figure 7. Comparison of dissolved methane and nitrogen concentrations in samples across the field area. Linear regression through data from the Parker-Hood cluster illustrates the negative correlation between dissolved methane and nitrogen in this area.

an approximation for the water table temperature that the dissolved gas in the groundwater was equilibrated with the atmosphere. Using this water table temperature, we calculate an initial dissolved nitrogen concentration for atmospheric-recharged groundwater of 14.5 mg/L and a $\delta^{15}\text{N}$ values near 0‰. Sample BS179A has a dissolved nitrogen concentration of 27.6 mg/L that is outside 2σ of the data set and may reflect addition of excess atmospheric nitrogen during recharge or contamination with atmospheric gas during sampling. With the exception of sample BS179A, samples outside the Parker-Hood cluster have dissolved nitrogen concentrations that average 17.5 ± 3.3 mg/L, which is slightly higher than, but within 1σ of groundwater recharged at 18 °C (Weiss, 1970).

Samples from the Parker-Hood cluster preserve dissolved nitrogen concentrations and $\delta^{15}\text{N}$ values of a wider range than observed outside the cluster and also preserve a negative correlation ($r^2 = 0.62$) whereby samples with the highest dissolved methane concentration have the lowest dissolved nitrogen concentration (Figure 7). Four samples (BS551, BS553, BS555, and BS355a) have dissolved nitrogen concentrations that are below 11 mg/L and cannot be explained through simple groundwater recharge equilibrated with atmosphere. These four samples also have the highest dissolved methane concentrations measured in the field area

(Figure 7), and three of these samples have dissolved nitrogen $\delta^{15}\text{N}$ values that are lower than expected for atmospheric-recharged groundwater (see Figure 6). Samples within the Parker-Hood cluster that have intermediate to nondetect dissolved methane concentrations also have dissolved nitrogen chemistries that are more typical of atmospheric-recharged groundwater (Figures 6 and 7).

5. Discussion of Dissolved Gas Processes and Transport of Stray Natural Gas

Collectively, measured alkane concentrations, $\delta^{13}\text{C}_{\text{methane}}$ values, and $\text{C1}/(\text{C2} + \text{C3})$ ratios of alkanes in shallow groundwater are consistent with the presence of stray natural gas in at least one cluster of groundwater wells on the border of Parker and Hood counties, and likely affected at least three groundwater wells in the southern Somervell cluster. A similar conclusion is reached by Wen et al. (2016) and Darrah et al. (2014) based on noble gas signatures. Sample locations outside these two clusters and throughout the entire field area have either nondetect or trace concentrations of dissolved methane. Locations with intermediate concentrations of dissolved methane also have nondetect concentrations of ethane and propane and low $\delta^{13}\text{C}_{\text{methane}}$ values that are consistent with contribution of methane from low-temperature microbial processes rather than migration of stray natural gas (Whiticar, 1999; Wolin & Miller, 1987; Zhang et al., 1998). In this section we couple measured dissolved alkane and nitrogen chemistry to test the hypothesis that dissolved nitrogen may add an additional source attribution technique and discern transport processes for stray natural gas. This approach of using dissolved nitrogen chemistry builds off dissolved noble gas chemistry studies by applying the same gas partitioning processes and calculations (Ballentine et al., 2002). Namely, we explore the effects of exsolution and dissolution of insoluble gases in two-phase systems and mixing between chemically distinct reservoirs. We directly compare results obtained with nitrogen chemistry to the noble gas research of Wen et al. (2016) that includes samples collected from the same wells in this study. In this way, the results of nitrogen chemistry can be validated against previously published noble gas methods. The observed relationship between methane concentration and dissolved nitrogen chemistry is considered with respect to three gas-water processes that will affect the $\delta^{15}\text{N}$ value and/or concentration of dissolved nitrogen in groundwater: (1) addition of excess nitrogen from external sources, (2) stripping of dissolved nitrogen from the aqueous phase into a gas phase, and (3) exchange or mixing of nitrogen between two nitrogen-bearing reservoirs. In addition to gas-water processes, we include effects associated with microbial denitrification which may have the coupled effect of (1) increasing the dissolved nitrogen concentration, (2) changing the $\delta^{13}\text{C}_{\text{methane}}$ value of residual methane, (3) changing the $\text{C1}/(\text{C2} + \text{C3})$ ratios of residual alkanes, and (4) changing the dissolved nitrate, sulfate, and dissolved inorganic carbon chemistry.

Excess nitrogen can be incorporated into shallow groundwater through the inclusion of atmospheric gas bubbles during groundwater recharge (Cey et al., 2009; Heaton & Vogel, 1981; Vogel et al., 1981) and from microbial denitrification (Knowles, 1982). The $\delta^{15}\text{N}$ value of atmospheric gas is close to 0‰ so the addi-

tion of excess atmospheric nitrogen would effectively increase the dissolved nitrogen concentration but not change the $\delta^{15}\text{N}$ value of atmosphere-recharged groundwater. The $\delta^{15}\text{N}$ value of nitrogen sourced from anaerobic microbial nitrate reduction is variable and dependent on the degree of denitrification and $\delta^{15}\text{N}$ value of the nitrate. Nitrate $\delta^{15}\text{N}$ values were not measured as part of this study, so it is not possible to fully assess the potential impact of this process. To the south of the field area, within the Cretaceous Edwards Aquifer, dissolved nitrate $\delta^{15}\text{N}$ values that range from +1.9‰ to +10‰ are reported with an average value of +6.2‰ (Kreitler & Browning, 1983). Dissolved nitrate concentrations ($n = 118$) measured in this study are generally low with only 28 samples having concentrations >5 mg/L and the majority of the samples ($n = 95$) having nondetect dissolved nitrate concentrations. The average dissolved nitrate concentration measured in this study is 1.5 mg/L and the maximum value measured within the Parker-Hood cluster is 4.4 mg/L. Complete reduction of an initial dissolved nitrate concentration of 4.4 mg/L having a $\delta^{15}\text{N}$ value of +6.2‰ would increase the $\delta^{15}\text{N}$ value and concentration of dissolved nitrogen in atmosphere-equilibrated groundwater to +0.4‰ and 15.5 mg/L (starting values of 14.5 mg/L and 0‰, respectively). Based on this estimate, the potential contribution of excess nitrogen through microbial denitrification is small and would not likely contribute significantly to the observed nitrogen chemistry in these groundwater samples. Also, the addition of excess nitrogen, either with an atmospheric or reduced nitrate $\delta^{15}\text{N}$ value, does not explain the range of data observed within the Parker-Hood cluster that includes lower than expected dissolved nitrogen concentrations and $\delta^{15}\text{N}$ values. This effect is important to consider, however, and is included as a possible pathway in our calculation, because it could have net effect of obscuring the process of nitrogen stripping that is described below.

Four groundwater wells sampled in the Parker-Hood cluster have dissolved nitrogen concentrations that are below 11.0 mg/L, which is more than 2σ different than the average dissolved nitrogen concentration measured outside the Park Hood cluster. These four groundwater wells also have the highest dissolved methane concentrations among the collected samples. Three of these samples have the lowest measured dissolved nitrogen $\delta^{15}\text{N}$ values in the data set. This correlation between high methane and low nitrogen dissolved concentrations suggests that groundwater with the lowest dissolved nitrogen concentrations were affected by the highest degree of mixing of stray natural gas. However, nitrogen stripping cannot solely account for the observed low $\delta^{15}\text{N}$ values in these three samples. Infiltration of a gas that has a low concentration of nitrogen may explain the resulting low dissolved nitrogen concentration in the groundwater (i.e., *stripping*). However, isotopic exchange between dissolved nitrogen and an infiltrating gas phase of nitrogen that also has a low $\delta^{15}\text{N}$ value is considered to explain the observed shift in dissolved nitrogen $\delta^{15}\text{N}$ values.

Stray natural gas in this field area is likely sourced from the Barnett Shale or Strawn Group. A critical difference between these two reservoirs is that natural gas from the Barnett Shale has lower nitrogen concentrations than natural gas from the Strawn Group. In the Barnett Shale nitrogen concentrations average $0.9 \pm 0.2\%$ with $\delta^{15}\text{N}$ values between -1.8% and -7% . In the Strawn Group natural gas has nitrogen concentrations that range from 3.9% to 4.3%. One $\delta^{15}\text{N}$ measurement from the Strawn Group production gas is -6.5% . Stripping or exsolution of dissolved nitrogen from groundwater is driven by compositional gradients and solubility constants whereby a large compositional disequilibrium between nitrogen-poor natural gas (gas phase) and nitrogen-rich atmosphere-equilibrated groundwater (aqueous phase) favors exsolution of dissolved nitrogen. Isotope exchange is driven by isotope concentration gradients and isotope solubility differences, but requires simultaneous exchange (i.e., exsolution and dissolution) between the gas and aqueous phases. In a closed system the chemical gradient at the gas-water interface would decrease through time, inhibiting further exsolution of dissolved gas. Continued stripping and exchange of dissolved nitrogen, therefore, is favored in either an open gas-phase system where stray natural gas continually flushes through the groundwater system, or in a closed system where a large gas to water ratio is established and maintained over long periods of time. To illustrate these concepts, we use an equilibrium mixing model to estimate the relative volumes of stray natural gas and groundwater necessary to develop the dissolved gas chemistry measured in this study.

The conceptual model is a finite volume of air saturated groundwater (dissolved nitrogen = 14.5 mg/L and $\delta^{15}\text{N} = +0.79\%$; dissolved methane = 0.01 mg/L) that is equilibrated with increasing volumes of natural gas. This mixing model is a proxy for natural gas stripping of dissolved nitrogen from air saturated groundwater. Two natural gas end members are investigated that are representative of the Barnett Shale (0.9% N_2 and $\delta^{15}\text{N} = -4.5\%$) and the Strawn Group (5% N_2 and $\delta^{15}\text{N} = -6.5\%$). Calculated volumetric mixing trends for these end members are illustrated in Figure 6. This is an equilibrium batch model that does not account for incomplete exchange or mixing or variations in reservoir temperatures and pressures; variables which are necessary

to develop a fully coupled gas transport model, but beyond the scope of this research. As such, this model is qualitative, yet provides important insight into geochemical trends of insoluble dissolved gas species and their stable isotope ratios as well as providing for comparison of the sensitivity to change for different geochemical indicators. Concentration of dissolved nitrogen in the mixing model is calculated using mass balance and Henry's Law constants at a constant temperature and hydrostatic pressure following equation (1):

$$\text{mols}_{\text{N}_2} = C_{\text{aq}} V_{\text{aq}} + C_{\text{gas}} V_{\text{gas}} \quad (1)$$

Where C_{aq} and C_{gas} are concentration of nitrogen in units of mols/L, and V_{aq} and V_{gas} are their respective volumes in units of liters. Substituting the Henry's Law relationship,

$$K_H = C_{\text{aq}}/C_{\text{gas}} \quad (2)$$

into equation (1) for C_{gas} where K_H is a dimensionless Henry's law constant for nitrogen (Wagner & Pruss, 1993; Weiss, 1970) and rearranging equation (1) to solve for dissolved nitrogen concentration yields equation (3):

$$C_{\text{aq}} = \frac{\text{mols}_{\text{N}_2}}{(V_{\text{aq}} + V_{\text{gas}}/K_H)} \quad (3)$$

Equation (3) is analogous to equation (2) of Ballentine et al. (1991), only solved for the concentration of a dissolved gas in an aqueous phase rather than mols of gas in the aqueous phase. $\delta^{15}\text{N}$ values are solved as a mass balance between two nitrogen end members assuming that solubility nitrogen isotope effects are insignificant (a small fractionation factor $\Delta^{15}\text{N}_{\text{gas-wat}} = +0.7\text{‰}$); this will have a minor effect on this model (Klots & Benson, 1963). Results of equation (3) coupled to nitrogen isotope mixing are illustrated in Figure 6 along with the dissolved nitrogen data from the Parker-Hood and Sumervell clusters and samples collected outside these clusters. Two gas:water mixing model trends are illustrated (solid lines): one for the Barnett Shale end member (0.9% N_2 and $\delta^{15}\text{N} = -4.5\text{‰}$) and one for the Strawn Group end member (5% N_2 and $\delta^{15}\text{N} = -6.5\text{‰}$).

Gas:water mixing model results demonstrate that natural gas with low nitrogen content, such as derived from the Barnett Shale, has a limited capacity to change the $\delta^{15}\text{N}$ value of dissolved nitrogen in groundwater. In contrast, natural gas with higher nitrogen content, such as that from the Strawn Group, does have the capacity to change both the concentration and $\delta^{15}\text{N}$ value of dissolved nitrogen in groundwater. Samples BS555, BS553, and BS551 from the Parker-Hood cluster have the lowest $\delta^{15}\text{N}$ values in the data set and are interpreted as being affected by isotopic exchange with stray gas. These three samples, however, do not fall on the mixing line calculated with the Strawn Group end member. Measured nitrogen concentrations and $\delta^{15}\text{N}$ values fall to the right of the Strawn Group mixing line, suggesting that more than simple natural gas and groundwater mixing has occurred. Whereas gas:water mixing ratios that average 1:10 are required to obtain the $\delta^{15}\text{N}$ values measured for BS551 and BS553 if the natural gas was sourced from the Strawn Group, the same degree of mixing results in considerably lower calculated dissolved nitrogen concentrations than are measured. Groundwater well BS555 has the lowest measured $\delta^{15}\text{N}$ value and would require a mixing ratio approaching 1:5 assuming natural gas that is representative of the Strawn Group. As with samples BS551 and BS553, measured dissolved nitrogen concentration for BS555 is higher than calculated with the mixing model. Calculated gas-water ratios, however, are consistent with gas:water ratios reported using noble gas mixing ratios from these wells (Wen et al., 2016). Specifically, mixing ratios calculated with $^{84}\text{Kr}/^{36}\text{Ar}$ and $^{132}\text{Xe}/^{36}\text{Ar}$ vary between 1:1 and 1:4 (Wen et al., 2016), consistent with the 1:5 estimate calculated here. Groundwater well BS355 has elevated methane concentration, but atmospheric nitrogen isotope values also have visible noble gas fractionations and display a lower gas:water ratio (1:16) calculated with noble gas ratios (Wen et al., 2016) that is consistent with gas:water ratios calculated here.

Although the gas:water mixing ratios estimated using measured $\delta^{15}\text{N}$ values are in agreement with mixing ratios calculated with noble gas ratios (Wen et al., 2016), the simple two-component gas:water stripping model does not accurately capture the measured dissolved nitrogen concentrations, which fall to the right of the Strawn Group mixing line (Figure 6). This suggests that either (1) a natural gas source far richer in nitrogen than the observed from the Strawn Group exists (e.g., 15% nitrogen source illustrated in Figure 6 for reference), (2) denitrification in methane-rich samples has added dissolved nitrogen gas that has a large $\delta^{15}\text{N}$ value, or (3) subsequent mixing of gas-stripped groundwater and atmosphere-equilibrated groundwater occurred. Lack of evidence for natural gas with such high concentrations of nitrogen in this region preclude the former hypothesis, and it is not further considered. Coupled anaerobic microbial oxidation, as described in the previous section, could add a third source of nitrogen and effectively shift the measured values from the mixing line. However, data presented here suggest that effect is minimal, and given the nitrate concentrations

in the Trinity aquifer, a maximum of 1 mg/L of dissolved nitrogen could be added through denitrification. The third scenario that natural gas-stripped groundwater is subsequently mixed with atmosphere-equilibrated groundwater is illustrated in Figure 6 as dotted mixing lines. Linear mixing between atmosphere-equilibrated groundwater and three points on the Strawn Group mixing line (1:10, 1:5, and 1:2 mixing ratios) are illustrated. This process reasonably explains the observed data and also may be expected for sampling water wells that are screened over large vertical intervals. We therefore favor this coupled process as a means of explaining the measured data in groundwater wells. Gas:water mixing ratios calculated using this additional mixing model are 1:2 for BS555, 1:5 for BS553, and 1:10 for BS551.

All the other collected groundwater samples, independent of the dissolved methane concentrations, have $\delta^{15}\text{N}$ values that are similar to atmospheric values and therefore do not appear to have experienced the degree of gas mixing as these three samples from the Parker-Hood cluster. The observed decrease in $\delta^{15}\text{N}$ does not appear to be possible with a lower nitrogen-bearing gas typical of the Barnett Shale. Similar conclusions are suggested for groundwater well BS199 (Kornacki & McCaffrey, 2014), which was not reanalyzed for dissolved nitrogen in this study. Combined, these data demonstrate that only three of the sampled groundwater wells preserve evidence of gas-phase transport of stray natural gas into shallow groundwater. These groundwater wells are known for gas lock of pumps and high levels of methane (personal communication with home owners). Of the other groundwater wells sampled that have high dissolved methane concentrations and lower than expected dissolved nitrogen concentrations, the measured $\delta^{15}\text{N}$ values of dissolved nitrogen argue against large influx of stray natural gas.

6. Conclusion

Dissolved alkane and nitrogen concentrations, and $\delta^{15}\text{N}_{\text{nitrogen}}$ and $\delta^{13}\text{C}_{\text{methane}}$ values measured within the Barnett Shale natural gas play suggest that stray natural gas infiltration is localized with a large cluster located near the border of Parker and Hood counties. Gas dryness and $\delta^{13}\text{C}_{\text{methane}}$ values clearly point to a thermogenic natural gas origin for the dissolved methane in the Parker-Hood cluster. However, these data alone are not sufficient to uniquely attribute this gas to the Barnett Shale, which is the target of hydraulic fracturing operations, because natural gas from the Strawn Group and Barnett Shale have similar alkane chemistries. Dissolved nitrogen chemistry measured in these groundwater samples an additional means to differentiate natural gas sources because of differences in nitrogen concentrations between the Strawn Group and Barnett Shale.

Results from our dissolved nitrogen model suggest that stray gas that infiltrated the groundwater in the Parker-Hood cluster likely contained higher nitrogen concentrations than measured for the Barnett Shale and are more typical of nitrogen concentrations measured from the Strawn Group. This conclusion is consistent with those of Darrah et al. (2014) and Wen et al. (2016) who, based on noble gas signatures within groundwater in Parker and Hood counties, concluded that stray natural gas in these groundwater wells is more likely sourced from the Strawn Group rather than the Barnett Shale. Gas to water mixing ratios as large as 1:2 are calculated for the most affected groundwater well (BS555) using dissolved nitrogen chemistry. The most likely scenario we envision for affected groundwater wells is localized transport of natural gas from the Strawn Group to the shallow groundwater aquifer that occurred during groundwater well drilling. Alternatively, isolated shallow natural gas reservoirs within the Strawn Group may be in contact with groundwater aquifers within the Trinity Group along the unconformable contact these rock units share.

Comparison of mixing model results for the alkane and nitrogen chemistry systems demonstrates their relative sensitivity to change. For example, groundwater equilibrated with atmospheric concentrations of nitrogen and methane that is mixed with natural gas with at least 5% nitrogen will require considerably less natural gas to shift its alkane chemistry to the thermogenic field (1:40 mixing; see Figure 2). With an equivalent 1:40 of mixing, the nitrogen system shows an appreciable decrease in dissolved nitrogen concentration (from 14 to 6.25 mg/L) but an insignificant decrease in the dissolved nitrogen $\delta^{15}\text{N}$ value. Gas to water mixing ratios larger than 1:20 are required to significantly decrease the $\delta^{15}\text{N}$ value in this example system. These model results illustrate the possible application of dissolved nitrogen chemistry to estimate volumetric gas:water mixing ratios and add another geochemical indicator for natural gas source attribution.

Acknowledgments

Funding for this project is provided by RPSEA (award 11122-56) through the Ultra-Deepwater and Unconventional Natural Gas and Other Petroleum Resources program authorized by the U.S. Energy Policy Act of 2005. The authors thank the technical support of Zac Hildebrand (Inform Environmental LLC) and Ruth Costley. The authors thank the many homeowners who graciously provided access to their groundwater wells. The data used are listed in the references and tables.

References

- Ashworth, J., Hopkins, J., & Board, T. W. D. (1995). Aquifers of Texas. no. 345 in Aquifers of Texas, Texas Water Development Board.
- Ball, M. M., & Perry, W. (1995). Bend Arch—Fort Worth basin province (045). DL Gautier, GL Dolton, KI Takahashi, and KL Varnes, eds.
- Ballentine, C. J., Burgess, R., & Marty, B. (2002). Tracing fluid origin, transport and interaction in the crust. *Reviews in Mineralogy and Geochemistry*, 47(1), 539–614.
- Ballentine, C., O'Nions, R., Oxburgh, E., Horvath, F., & Deak, J. (1991). Rare gas constraints on hydrocarbon accumulation, crustal degassing and groundwater flow in the Pannonian basin. *Earth and Planetary Science Letters*, 105(1), 229–246. [https://doi.org/10.1016/0012-821X\(91\)90133-3](https://doi.org/10.1016/0012-821X(91)90133-3)
- Barker, J. F., & Fritz, P. (1981). Carbon isotope fractionation during microbial methane oxidation. *Nature*, 293, 289–291.
- Bernard, B., Brooks, J. M., & Sackett, W. M. (1977). A geochemical model for characterization of hydrocarbon gas sources in marine sediments. In *Offshore Technology Conference* (pp. 425–438).
- Brown, L. F. Jr. (1973). Cratonic basins: Terrigenous clastic models: in Guidebook No. 14, Pennsylvanian Depositional Systems in North Central Texas. *Bureau of Economic Geology*, 10–30.
- Cey, B. D., Hudson, G. B., Moran, J. E., & Scanlon, B. R. (2009). Evaluation of noble gas recharge temperatures in a shallow unconfined aquifer. *Groundwater*, 47(5), 646–659.
- Chaudhuri, S., & Ale, S. (2013). Characterization of groundwater resources in the Trinity and Woodbine aquifers in Texas. *Science of The Total Environment*, 452-453, 333–348. <https://doi.org/10.1016/j.scitotenv.2013.02.081>
- Christian, K. M., Lautz, L. K., Hoke, G. D., Siegel, D. I., Lu, Z., & Kessler, J. (2016). Methane occurrence is associated with sodium-rich valley waters in domestic wells overlying the Marcellus shale in New York State. *Water Resources Research*, 52, 206–226. <https://doi.org/10.1002/2015WR017805>
- Darrah, T. H., Vengosh, A., Jackson, R. B., Warner, N. R., & Poreda, R. J. (2014). Noble gases identify the mechanisms of fugitive gas contamination in drinking-water wells overlying the Marcellus and Barnett shales. *Proceedings of the National Academy of Sciences*, 111(39), 14,076–14,081. <https://doi.org/10.1073/pnas.1322107111>
- Darvari, R., Nicot, J.-P., Scanlon, B. R., Mickler, P., & Uhlman, K. (2017). Trace element behavior in methane-rich and methane-free groundwater in north and east Texas. *Groundwater*. <https://doi.org/10.1111/gwat.12606>
- Eltchlagler, K. K., Hawkins, J. W., Ehler, W. C., Baldassare, F., & Baldassare, F. (2001). Technical measures for the investigation and mitigation of fugitive methane hazards in areas of coal mining (US Dept of the Interior, Office of Surface Mining Reclamation and Enforcement, Pittsburgh) (pp. 124).
- Ettwig, K. F., Butler, M. K., Le Paslier, D., Pelletier, E., Mangenot, S., Kuypers, M. M., et al. (2010). Nitrite-driven anaerobic methane oxidation by oxygenic bacteria. *Nature*, 464(7288), 543–548.
- Fuex, A. (1980). Experimental evidence against an appreciable isotopic fractionation of methane during migration. *Physics and Chemistry of the Earth*, 12, 725–732.
- Gilfillan, S. M., Lollar, B. S., Holland, G., Blagburn, D., Stevens, S., Schoell, M., et al. (2009). Solubility trapping in formation water as dominant CO₂ sink in natural gas fields. *Nature*, 458, 614–618.
- Golding, S. D., Boreham, C. J., & Esterle, J. S. (2013). Stable isotope geochemistry of coal bed and shale gas and related production waters: A review. *International Journal of Coal Geology*, 120, 24–40.
- Grossman, E. L., Coffman, B. K., Fritz, S. J., & Wada, H. (1989). Bacterial production of methane and its influence on ground-water chemistry in east-central Texas aquifers. *Geology*, 17(6), 495–499.
- Heaton, T., & Vogel, J. (1981). "Excess air" in groundwater. *Journal of Hydrology*, 50, 201–216.
- IHS (2015). Well completion and production reports supplied by the Enerdeq database. Retrieved from <https://www.ih.com/products/oil-gas-tools-enerdeq-browser.html>
- Jackson, R. B., Vengosh, A., Darrah, T. H., Warner, N. R., Down, A., Poreda, R. J., et al. (2013). Increased stray gas abundance in a subset of drinking water wells near Marcellus shale gas extraction. *Proceedings of the National Academy of Sciences*, 110(28), 11,250–11,255. <https://doi.org/10.1073/pnas.1221635110>
- Jarvie, D. M., Hill, R. J., Ruble, T. E., & Pollastro, R. M. (2007). Unconventional shale-gas systems: The Mississippian Barnett shale of North-Central Texas as one model for thermogenic shale-gas assessment. *AAPG Bulletin*, 91(4), 475–499.
- Jenden, P., Kaplan, I., Poreda, R., & Craig, H. (1988). Origin of nitrogen-rich natural gases in the California Great Valley: Evidence from helium, carbon and nitrogen isotope ratios. *Geochimica et Cosmochimica Acta*, 52(4), 851–861. [https://doi.org/10.1016/0016-7037\(88\)90356-0](https://doi.org/10.1016/0016-7037(88)90356-0)
- Kampbell, D. H., & Vandegrift, S. A. (1998). Analysis of dissolved methane, ethane, and ethylene in ground water by a standard gas chromatographic technique. *Journal of Chromatographic Science*, 36(5), 253–256.
- Klots, C., & Benson, B. (1963). Solubilities of nitrogen, oxygen, and argon in distilled water. *Journal of Marine Research*, 21, 48–57.
- Knowles, R. (1982). Denitrification. *Microbiological Reviews*, 46(1), 43–70.
- Kornacki, A. S., & McCaffrey, M. (2014). Monitoring the active migration and biodegradation of natural gas in the trinity troupe aquifer at the Silverado development in southern Parker County, Texas. AAPG 2014 Annual Conference.
- Kreitler, C. W., & Browning, L. A. (1983). Nitrogen-isotope analysis of groundwater nitrate in carbonate aquifers: Natural sources versus human pollution, V.T. Stringfield symposium—Processes in Karst hydrology. *Journal of Hydrology*, 61(1), 285–301. [https://doi.org/10.1016/0022-1694\(83\)90254-8](https://doi.org/10.1016/0022-1694(83)90254-8)
- Krooss, B., Littke, R., Müller, B., Frielingsdorf, J., Schwöcher, K., & Idiz, E. (1995). Generation of nitrogen and methane from sedimentary organic matter: Implications on the dynamics of natural gas accumulations. *Chemical Geology*, 126(3), 291–318.
- Loucks, R. G., & Ruppel, S. C. (2007). Mississippian Barnett shale: Lithofacies and depositional setting of a deep-water shale-gas succession in the Fort Worth basin, Texas. *AAPG Bulletin*, 91(4), 579–601.
- Lu, J., Larson, T. E., & Smyth, R. C. (2015). Carbon isotope effects of methane transport through Anahuac shale—A core gas study. *Journal of Geochemical Exploration*, 148, 138–149.
- Márquez, G., Escobar, M., Lorenzo, E., Gallego, J., & Tocco, R. (2013). Using gas geochemistry to delineate structural compartments and assess petroleum reservoir-filling directions: A Venezuelan case study. *Journal of South American Earth Sciences*, 43, 1–7.
- Mingram, B., Hoth, P., & Harlov, D. E. (2003). Nitrogen potential of Namurian shales in the North German basin. *Journal of Geochemical Exploration*, 78, 405–408.
- Molofsky, L. J., Connor, J. A., Wylie, A. S., Wagner, T., & Farhat, S. K. (2013). Evaluation of methane sources in groundwater in northeastern Pennsylvania. *Groundwater*, 51(3), 333–349.
- Molofsky, L. J., Richardson, S. D., Gorody, A. W., Baldassare, F., Black, J. A., McHugh, T. E., & Connor, J. A. (2016). Effect of different sampling methodologies on measured methane concentrations in groundwater samples. *Groundwater*, 54(5), 669–680. <https://doi.org/10.1111/gwat.12415>

- Montgomery, S. L., Jarvie, D. M., Bowker, K. A., & Pollastro, R. M. (2005). Mississippian Barnett shale, Fort Worth basin, North-Central Texas: Gas-shale play with multi-trillion cubic foot potential. *AAPG Bulletin*, *89*(2), 155–175.
- Moritz, A., Helie, J.-F., Pinti, D. L., Larocque, M., Barnette, D., Retaillieu, S., et al. (2015). Methane baseline concentrations and sources in shallow aquifers from the shale gas-prone region of the St. Lawrence lowlands (Quebec, Canada). *Environmental Science & Technology*, *49*(7), 4765–4771.
- Nicot, J. P. (2013). Flow and salinity patterns in the low-transmissivity upper Paleozoic aquifers of North-Central Texas. *Gulf Coast Association of Geological Societies Journal*, *2*, 53–67.
- Nicot, J. P., Mickler, P., Larson, T., Clara Castro, M., Darvari, R., Uhlman, K., & Costley, R. (2017). Methane occurrences in aquifers overlying the Barnett shale play with a focus on Parker County, Texas. *Groundwater*, *55*(4), 469–481.
- Nicot, J. P., Scanlon, B. R., Reedy, R. C., & Costley, R. A. (2014). Source and fate of hydraulic fracturing water in the Barnett shale: A historical perspective. *Environmental Science & Technology*, *48*(4), 2464–2471.
- Nordstrom, P. L. (1982). Occurrence, availability, and chemical quality of ground water in the cretaceous aquifers of North Central Texas.
- Osborn, S. G., Vengosh, A., Warner, N. R., & Jackson, R. B. (2011). Methane contamination of drinking water accompanying gas-well drilling and hydraulic fracturing. *Proceedings of the National Academy of Sciences*, *108*(20), 8172–8176. <https://doi.org/10.1073/pnas.1100682108>
- Pollastro, R. M., Jarvie, D. M., Hill, R. J., & Adams, C. W. (2007). Geologic framework of the Mississippian Barnett shale, Barnett-Paleozoic total petroleum system, Bend Arch, Fort Worth basin, Texas. *AAPG Bulletin*, *91*(4), 405–436.
- Prinzhofer, A., Mello, M. R., & Takaki, T. (2000). Geochemical characterization of natural gas: A physical multivariable approach and its applications in maturity and migration estimates. *AAPG Bulletin*, *84*(8), 1152–1172.
- Rodriguez, N. D., & Philp, R. P. (2010). Geochemical characterization of gases from the Mississippian Barnett shale, Fort Worth basin, Texas. *AAPG Bulletin*, *94*(11), 1641–1656.
- Rostron, B., & Arkadaskiy, S. (2014). Fingerprinting “stray” formation fluids associated and production with hydrocarbon exploration and production. *Elements*, *10*(4), 285–290. <https://doi.org/10.2113/gselements.10.4.285>
- Schoell, M. (1980). The hydrogen and carbon isotopic composition of methane from natural gases of various origins. *Geochimica et Cosmochimica Acta*, *44*(5), 649–661.
- Siegel, D. I., Azzolina, N. A., Smith, B. J., Perry, A. E., & Bothun, R. L. (2015). Methane concentrations in water wells unrelated to proximity to existing oil and gas wells in northeastern Pennsylvania. *Environmental Science & Technology*, *49*(7), 4106–4112.
- Solomon, D., Hunt, A., & Poreda, R. (1996). Source of radiogenic helium 4 in shallow aquifers: Implications for dating young groundwater. *Water Resources Research*, *32*(6), 1805–1813.
- Stumm, W., & Morgan, J. J. (2012). *Aquatic chemistry: Chemical Equilibria and Rates in Natural Waters* (3rd ed.). New York: John Wiley.
- Thompson, H. (2012). Fracking boom spurs environmental audit. *Nature*, *485*, 556–557.
- Torres, M. E., Mix, A. C., & Rugh, W. D. (2005). Precise $\delta^{13}\text{C}$ analysis of dissolved inorganic carbon in natural waters using automated headspace sampling and continuous-flow mass spectrometry. *Limnology & Oceanography: Methods*, *3*, 349–360.
- Valentine, D. L., & Reeburgh, W. S. (2000). New perspectives on anaerobic methane oxidation. *Environmental Microbiology*, *2*(5), 477–484. <https://doi.org/10.1046/j.1462-2920.2000.00135.x>
- Vogel, J., Talma, A., & Heaton, T. (1981). Gaseous nitrogen as evidence for denitrification in groundwater. *Journal of Hydrology*, *50*, 191–200.
- Wagner, W., & Pruss, A. (1993). International equations for the saturation properties of ordinary water substance. Revised according to the international temperature scale of 1990. Addendum to Journal of Physical and Chemical Reference Data 16, 893 (1987). *Journal of Physical and Chemical Reference Data*, *22*(3), 783–787.
- Waldron, S., Scott, E. M., Vihermaa, L. E., & Newton, J. (2014). Quantifying precision and accuracy of measurements of dissolved inorganic carbon stable isotopic composition using continuous-flow isotope-ratio mass spectrometry. *Rapid Communications in Mass Spectrometry*, *28*(10), 1117–1126. <https://doi.org/10.1002/rcm.6873>
- Weiss, R. (1970). The Solubility of Nitrogen, Oxygen and Argon in Water and Seawater. *Deep-Sea Research*, *17*, 721–735.
- Wen, T., Castro, M. C., Ellis, B. R., Hall, C. M., & Lohmann, K. C. (2015). Assessing compositional variability and migration of natural gas in the Antrim shale in the Michigan basin using noble gas geochemistry. *Chemical Geology*, *417*, 356–370.
- Wen, T., Castro, M. C., Nicot, J.-P., Hall, C. M., Larson, T., Mickler, P. J., & Darvari, R. (2016). *Methane Sources and Migration Mechanisms in Shallow Groundwaters in Parker and Hood Counties, Texas—A Heavy Noble Gas Analysis* (Vol. 50, pp. 12,012–12,021).
- Wen, T., M. C. Castro, J.-P. Nicot, Hall, C. M., Pinti, D. L., Mickler, P., et al. (2017). Characterizing the noble gas isotopic composition of the Barnett shale and Strawn group and constraining the source of stray gas in the Trinity aquifer, North-Central Texas. *Environmental Science & Technology*, *51*(11), 6533–6541. <https://doi.org/10.1021/acs.est.6b06447>
- Whiticar, M. J. (1999). Carbon and hydrogen isotope systematics of bacterial formation and oxidation of methane. *Chemical Geology*, *161*(1), 291–314.
- Wolin, M. J., & Miller, T. L. (1987). Bioconversion of organic carbon to CH_4 and CO_2 . *Geomicrobiology Journal*, *5*(3-4), 239–259. <https://doi.org/10.1080/01490458709385972>
- Zhang, C., Grossman, E. L., & Ammerman, J. W. (1998). Factors influencing methane distribution in Texas ground water. *Groundwater*, *36*(1), 58–66. <https://doi.org/10.1111/j.1745-6584.1998.tb01065.x>